Sensitivity of enhanced vertical resolution in the operational Global Forecast System (GFS) T1534 on the short to medium range forecast of Indian summer monsoon

Malay Ganai[1] · R. Phani Murali Krishna[1] · Snehlata Tirkey[1] · Parthasarathi Mukhopadhyay[1]

Abstract

The sensitivity of increased vertical resolution in the present operational global forecast system (GFS) at T1534 (~12.5 km) model on the short to medium range forecast of Indian summer monsoon (ISM) is investigated during June to September for year of 2020. The present operational GFS model has 64 hybrid vertical layers with model top at 0.27 hPa (~54 km) which is enhanced to 128 hybrid levels with model top at 0.01 hPa (~80 km). The results reveal that GFS L128 (EXPT) shows improved mean precipitation distribution over the central India, Indo-Gangetic Plain, and southern Peninsula region compared to GFS L64 (CTRL) forecast. It is found that CTRL forecast predicts around 20% excess rainfall over the central India region which is reduced to 3% excess in EXPT forecast. However, EXPT shows excess rainfall (23%) over the northeast India, Himalayan foothills, Western Ghats (WGs) and Bay of Bengal (BoB) region compared to both observation and CTRL forecast (19.5%). The precipitation probability distribution function (PDF) shows notable improvement in the heavy to extreme category rainfall in EXPT for all the lead times over the central India region. The improvement in the total rainfall over the central Indian landmass region is likely contributed by the realistic convective and large-scale rainfall in EXPT forecast. The enhanced vertical resolution in EXPT likely helped in resolving the vertical moisture distribution resulting better moist-convective feedback in the atmospheric column. Moreover, skill score analysis based on precipitation clearly brings out the better model fidelity with enhanced vertical levels in EXPT forecast over the central Indian landmass region. In addition to daily scale, diurnal cycle of precipitation shows realistic phase and amplitude over the above region in EXPT forecast compared to CTRL. Finally, the fidelity of increased vertical velocity is tested for few extreme rainfall cases and it is found that EXPT is able to retain the intensity of the extreme rainfall with longer lead times over that of CTRL forecast. With the increasing trend in extreme rainfall events over India, the EXPT forecast shows its potential in improving heavy rainfall forecasting during summer monsoon. Additionally, the enhance skill of predicting extreme rainfall events is crucial for several societal applications, such as businesses and energy trading sectors increasingly rely on weather forecasts. Therefore, the present study is not only beneficial for the current operational prediction system but also paves the way for further enhancements.

1 Introduction

The Indian summer monsoon rainfall (ISMR), measured by rainfall from June to September (JJAS) over the Indian subcontinent, plays a major driving force for agricultural productivity, water resource management and many other socio-economic aspects of the country. The JJAS summer monsoon season alone contributes more than 75% of the annual rainfall in India. The floods and droughts associated with year-to-year monsoon rainfall variations exceeding 10% of the long-term mean cause severe distress to the region's people (Gadgil and Gadgil 2006). Therefore, accurate prediction of monsoon precipitation is essential from the societal perspective. This is particularly important considering the fact that studies (Goswami et al. 2006; Rajeevan et al. 2008; Roxy et al. 2017) have highlighted the increasing trend of extreme rainfall over the Indian subcontinent. Further, the intensity of extreme precipitation is enhanced in recent

✉ Malay Ganai
 malayganai58@gmail.com; malay.cat@tropmet.res.in

[1] Ministry of Earth Sciences, Indian Institute of Tropical Meteorology, Dr. Homi Bhabha Road, Pune 411008, India

decades (Sen Roy and Balling 2004; Nageswararao et al. 2016; Barde et al. 2020) during different seasons in India. The economic loss caused by floods in India is about $3 billion per year, which is about 10% of the global financial losses, according to the International Disaster Database (http://www.emdat.be).

The prediction skill of numerical weather models has improved in recent years mainly due to better initialization, increased resolution, and realistic model physics. Over the past decades, the numerical models' horizontal resolution has increased globally, mainly due to improved computing facilities. Various studies (Mahlman and Umscheid 1987; Kiehl and Williamson 1991; Hack et al. 2006; Manganello et al. 2012) have highlighted the importance of horizontal resolution in model simulation due to better representation of orography, vegetation cover, land–ocean coastlines and associated nonlinear processes. The pace of the increased horizontal resolution in numerical models has been relatively fast in recent decades. However, the enhancement in the vertical resolution remains slow in major operational weather prediction centres. For instance, the National Centers for Environmental Prediction (NCEP) Global Forecast System (GFS) model had been using 64 hybrid vertical levels for 18 years (2002–2020) until recently; it changed to 127 levels. Interestingly, during this period, the horizontal resolution increased from 55 to 13 km in the NCEP GFS model. Further details can be found at https://www.emc.ncep.noaa.gov/gmb/STATS /html/model_changes.html. Lindzen and Fox-Rabinovitz (1989) first indicated that physical consistency of horizontal and vertical resolutions in the design of numerical models is essential for weather prediction and that lack of consistency may lead to generation of noise and affect the predictability. Further, Lee et al. (2019) have documented (Table 1 in their paper) the vertical resolution updates in various operational centers across the globe. Mass et al. (2002) have reported that horizontal and vertical resolutions influence the atmosphere's dynamical and physical processes and modulate the uncertainties in these processes because a finer-scale model grid can resolve small-scale features. Several studies have carried out the impact of increased vertical resolution in simulating synoptic systems. Among them, Zhang and Wang (2003) showed using Pennsylvania State University/National Center for Atmospheric Research (PSU/NCAR) mesoscale model that higher vertical resolution in the lower-level leads to efficient intensification of a hurricane. They concluded that higher vertical and finer horizontal resolutions are desirable for realistic simulation of tropical storm intensity. Similar result was also echoed by Bhaskar Rao et al. (2010) where they have shown the finer vertical resolution improves the tropical cyclone intensification and better structure in terms of eye and eyewall of tropical cyclone using NCAR mesoscale model. Further, they found that increased vertical resolution

Table 1 Various statistics (mean, spatial correlation coefficient (CC), root mean square error (RMSE), and standard deviation) are calculated based on observed and model forecasted rainfall over continental Indian region for different lead times

	Lead day	Mean (mm/day)	CC	RMSE (mm/day)	Standard Deviation (mm/day)
IMD-GPM		7.7			10.7
CTRL	Day-1	9.2	0.55	17.1	8.8
EXPT	Day-1	9.5	0.44	18.1	9.4
CTRL	Day-3	8.9	0.55	18.2	9.4
EXPT	Day-3	10.2	0.51	21.8	11.8
CTRL	Day-5	9.4	0.52	18.6	9.1
EXPT	Day-5	10.7	0.50	22.0	11.4
CTRL	Day-8	9.6	0.48	19.0	9.0
EXPT	Day-8	10.8	0.49	22.7	12.1

at the lower level leads to improvement in the prediction of vertical shear of the horizontal wind. Apart from the above synoptic systems, higher vertical resolution can influence the stratospheric forecast, as Charron et al. (2012) demonstrated. They have shown that increasing the model top height from 10 hPa to 0.1 hPa in the Canadian Meteorological Centre leads to significant improvement in the stratospheric and medium-range tropospheric forecast skill.

In addition to the above studies, Ruti et al. (2006) showed the impact of increased vertical resolution in the ECHAM4 climate model. They reported improvements in the tropical dynamical fields and precipitation distribution due to improved cloud structure. Further, they noted that in a higher vertical resolution model, the convective parameterization starts to show cumulus congestus clouds. Another study by Bauer et al. (2013) demonstrated that increased vertical resolution has a mixed impact on the tropics and extratropics medium range forecast in ECMWF model. The results are likely due to various sensitivities to vertical resolution in the dynamics and model physical parameterization. The impact of vertical resolution on the Indian summer monsoon in the climate model has been studied by Abhik et al. (2014) using ECMWF model. They demonstrated that increased vertical resolution leads to better simulation of summer intraseasonal oscillation. Over India, the medium range weather forecast started at National Centre for Medium Range Weather Forecast (NCMRWF) in 1994 using the T80L18 global data assimilation and forecasting system. Since then, with the improvement in the observational data network, data assimilation, model development and computational facilities, the skill of the operational forecast model has been enhanced over the years. The horizontal resolution of the Global Forecasting System (GFS) operational forecast model in India has increased from T382 (~38 km) to T574 (~27 km) to T1534 (~12.5 km) for over a decade time

period. However, the vertical resolution has remained at L64 (64 hybrid vertical levels) in GFS for all these years. Mukhopadhyay et al. (2019) demonstrated the forecast skill of the current operational GFS T1534L64 model forecast over the Indian summer monsoon region. It is noted that the high-resolution model has predicted the mean monsoon features (namely precipitation, circulation, dynamical processes, etc.) reasonably well. However, it considerably underestimates the heavier category rainfall and overestimates the lighter category rainfall for all the lead times over the Indian sub-continent. Further, studies (Goswami et al. 2006; Rajeevan et al. 2008; Roxy et al. 2017) have highlighted the increasing trend of extreme rainfall events over the Indian region. Therefore, keeping the above studies and issues in mind, in the present study, for the first time, an attempt is taken to increase the vertical resolution of the present operational GFS model from L64 to L128 hybrid vertical levels. The primary objective of the current manuscript is to assess the sensitivity of increased vertical resolution in GFS on the forecast of Indian summer monsoon features and its potential in predicting extreme rainfall events over Indian region. Model details, data and methodology are given in Sect. 2. Results and discussions are provided in Sect. 3 and Sect. 4 summarizes and concludes the study.

2 Model details, data and methodology

Over the Indian region, NCEP GFS version 14.1.0 with spectral horizontal resolution of T1534 (~ 12.5 km) with 64 hybrid sigma-pressure levels (top layer 0.27 hPa) is employed for short to medium range weather forecast system. The dynamical core of the model is based on semi-implicit Semi-Lagrangian (SL) discretization approach (Sela 2010), while the physics is done in the linear, reduced gaussian grid. The present operational GFST1534 uses scale aware simplified Arakawa-Schubert deep convection scheme (Han and Pan 2011; Han et al. 2017) and mass-flux based shallow convection scheme (Han and Pan 2011). The cloud microphysics scheme is based on Zhao and Carr (1997) and Sundqvist et al. (1989), which uses only one prognostic cloud species (total cloud water). Further, the model utilizes gravity wave drag following Alpert et al. (1988); Kim and Arakawa (1995), mountain blocking (Lott and Miller 1997) and stationary convective-forced gravity wave drag (Chun and Baik 1998). The planetary boundary layer (PBL) scheme uses hybrid Eddy-diffusivity mass flux vertical mixing scheme (Han and Pan 2011; Han et al. 2016). Further model details about the model physics can be found at Ganai et al. (2021). In the present study, the hybrid vertical layers are increased from 64 (https://www.emc.ncep.noaa.gov/gmb/wx24fy/misc/GFS127_profile/hyblev_gfs64.txt) to 128 levels which are similar to NCEP's present

operational GFS version 16 model (https://www.emc.ncep.noaa.gov/gmb/wx24fy/misc/GFS127_profile/hyblev_gfsC128.txt). With the increase in the vertical resolution in L128, the vertical grid spacing has decreased throughout the atmosphere. The higher number of vertical levels near the surface in L128 compared to L64 gives the reduced lowest model level height of around 20 m than 45 m in L64 in the GFS T1534 model. The model top level is increased from 0.27 hPa (~ 54 km) in L64 to 0.01 hPa (~ 80 km) in L128. In the present study, two GFS T1534 model forecasts are used, one with L64 levels (CTRL hereafter) and the other with L128 levels (EXPT hereafter). It is worth to mention that except vertical resolution, all the model components are remained same for both CTRL and EXPT. The model forecast is run daily for 10 days, and the output is stored at every 3-h interval at 12.5 km regular latitude–longitude grid for the year of 2020, June to September (JJAS) months. These models run are performed at the Ministry of Earth Sciences high-performance computing system "Pratyush" at the Indian Institute of Tropical Meteorology (IITM), Pune, India. The initial conditions for the forecast are generated by the National Centre for Medium Range Weather Forecasting (NCMRWF) using the NCEP-based ensemble Kalman filter (EnKF) component of hybrid global data assimilation system (GDAS) cycle, which contains more Indian data. More details about the NCMRWF data assimilation system are documented by Prasad et al. (2016).

Several observation datasets based on satellite estimates and reanalysis products are utilized to validate the model forecast. The precipitation data is taken from India Meteorological Department (IMD) and Global Precipitation Measurement (GPM) daily merged data (Mitra et al. 2014) for the year 2020 during JJAS season. The reanalyses products (wind, relative humidity, vertical velocity, temperature) is utilized from the fifth generation of ECMWF atmospheric reanalyses (ERA5) products (Hersbach and Dee 2016) over Indian summer monsoon region for JJAS-2020. For the diurnal cycle of rainfall, the Integrated Multi-satellitE Retrievals for GPM (IMERG) (Huffman et al. 2019) satellite-based data is used for the year of 2020 JJAS season.

In the present study, the 24-h accumulated rainfall is calculated from 3 hourly (03 UTC of the previous day to 03 UTC of forecast valid day) forecast data over the Indian region for both models during JJAS of the year 2020. The JJAS mean precipitation is calculated based on one year (2020) of datasets for day-1, day-3, day-5 and day-8 forecast lead time. Several statistical parameters namely, spatial correlation coefficient, root mean square error (RMSE) are computed for both models with respect to observation. Moreover, analysis of bias, rainfall probability distribution function (PDF), cumulative distribution function (CDF), regional Hadley circulation, vertical profiles of various dynamical and thermodynamical parameters etc. are calculated for both

observation and model forecasts for various lead times. In order to examine the forecast skill of EXPT, various skill scores are evaluated in Sect. 3.3. The computation of Bias score (B) and Equitable Threat Score (ETS) are carried out based on a contingency table. The contingency table categorizes the observation and forecast into hits, 'a', false alarms, 'b', miss, 'c' and correct negatives 'd' with respect to a particular threshold. Based on these categories the Bias Score and ETS are calculated (Wilks 2011).

$$B = \frac{a+b}{a+c} \tag{1}$$

$$ETS = \frac{a - a_{ref}}{a + b + c - a_{ref}} \tag{2}$$

A Bias Score (B) of 1 implies a perfect forecast, greater than 1 indicates overforecasting and less than 1 signifies underforecasting. The ETS varies between -1/3 to 1 with closer to 1 suggests better forecast. Finally, the 3 hourly precipitation diurnal cycle is also computed for observation and models over the various regions over India as depicted in Fig. 1.

3 Results and discussions

3.1 Seasonal mean precipitation distribution

To start with, the Indian summer monsoon (ISM) precipitation distribution is investigated for both the models over the ISM region (Fig. 2) during JJAS of the year 2020. The

observed IMD-GPM merged precipitation indicates that major precipitation occurs over the central India (CI), Western Ghats, Bay of Bengal (BoB), northeast India, and the Himalayan foothills region (Fig. 2a). On the contrary, the northwest India and the southern peninsula received the least amount of rainfall during summer of 2020. The model biases in CTRL and EXPT are shown in Fig. 2b and c, respectively. The CTRL forecast appears to overestimate the precipitation distribution throughout the Indian landmass region for all the lead times during the 2020 summer season (Fig. 2b). Among all the landmass regions, CI, northeast India and the region of the Himalayan foothills have a considerable positive rainfall bias in CTRL forecast. Similar wet bias is also noted in CTRL simulation in other years as shown by Mukhopadhyay et al. (2019) and Ganai et al. (2021). However, in the EXPT forecast, it is seen that the excess precipitation overestimation in CTRL simulation is reduced over the majority of the Indian landmass regions (Fig. 2c). Particularly, the noteworthy improvement is seen over the CI, southern peninsula and Indo-Gangetic plain areas. However, over the northeast India and Himalayan foothills region, EXPT shows considerable precipitation overestimation during JJAS of 2020 (Fig. 2c) for all the lead time. Additionally, the positive precipitation bias is noted over the Western Ghats (WGs) and BoB region from day-3 lead time in EXPT forecast. Interestingly, both the models show a dry bias over the head BoB region for Day-1 lead time. These results are further evident in the model-to-model comparison as shown in Fig. 2c. Major precipitation overestimation is noted over the Himalayan foothills region, WGs, BoB, and northeast India in EXPT

Fig.1 Selected boxes over the Indian land region, Bay of Bengal and equatorial Indian Ocean (EIO) to calculate the diurnal cycle of rainfall in Fig. 15
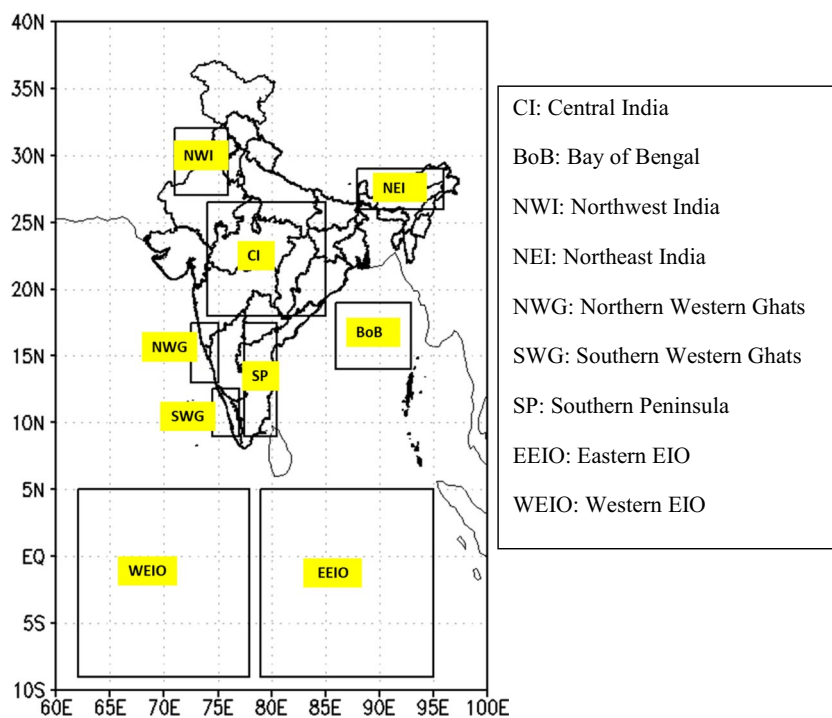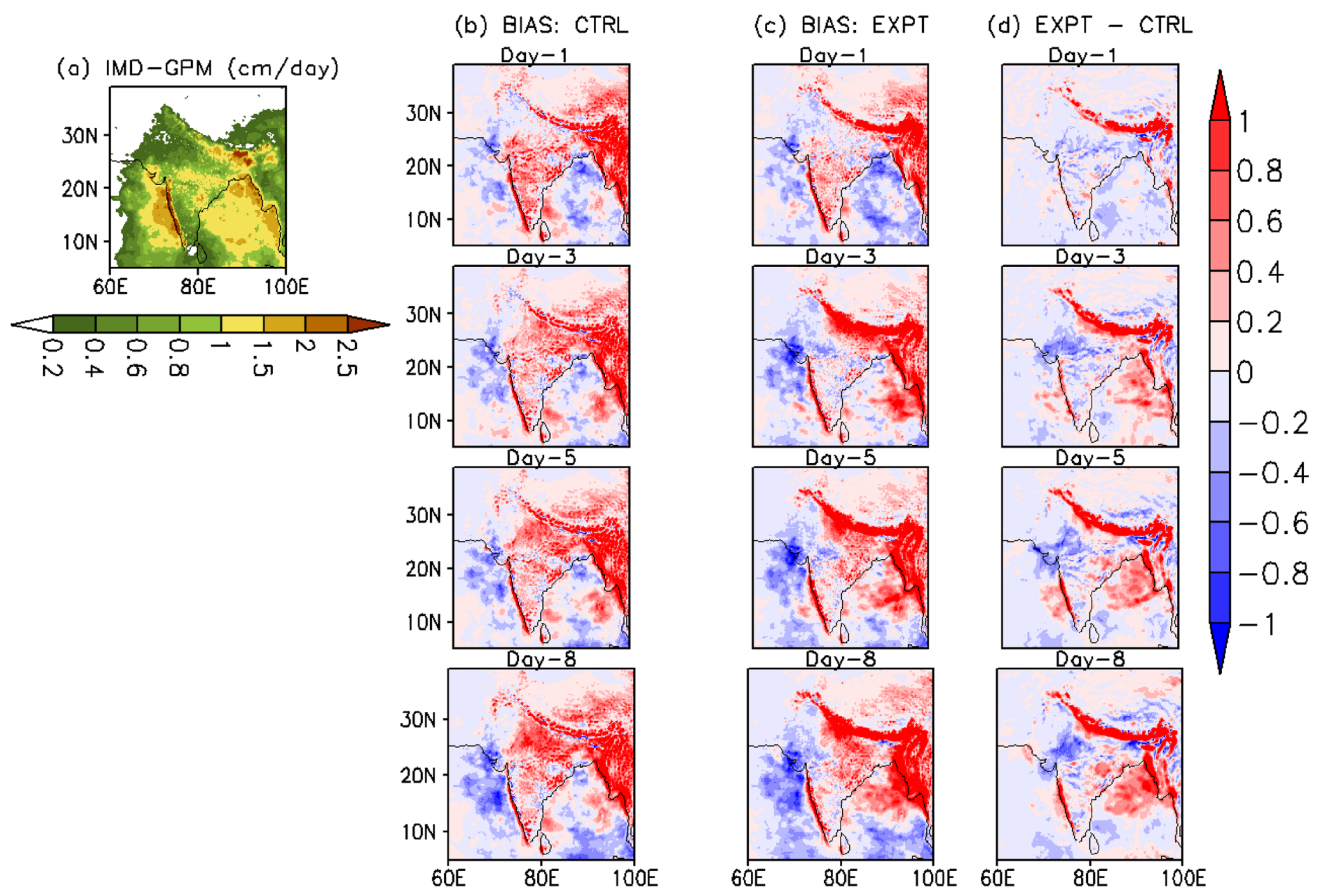
Fig.2 (**a**) JJAS mean rainfall (cm day^{-1}) of IMD-GPM merged data during 2020. The rainfall bias in (**b**) CTRL and (**c**) EXPT with respect to observation, (**d**) in EXPT with respect to CTRL for day-1, day-3, day-5, and day-8 lead time are shown

compared to the CTRL region. From the above analyses, it is noted that EXPT shows better precipitation distribution over the CI region. In contrast, gross overestimation is reported over the WGs, BoB, northeast and Himalayan region compared to CTRL. To establish the above facts, various statistical parameters are calculated over the Indian landmass and CI region separately, as shown in Table 1 and Table 2, respectively. Over the Indian subcontinent region, it is found that the mean, spatial correlation coefficient (CC), root mean square error (RMSE) and standard deviation of precipitation are better in CTRL as compared to the EXPT forecast for all the lead times for JJAS of the year 2020 (Table 1). It suggests better precipitation distribution over Indian subcontinent in CTRL forecast compared to EXPT. On the contrary, EXPT sensitivity study shows better performance in forecasting the above statistics (except standard deviation) over the CI region than CTRL (Table 2). Therefore, it is evident from the above analyses that precipitation biases in the northeast India, Himalayan foothills, WGs regions in EXPT forecast largely influence the seasonal mean all India rainfall amount and other statistics as shown in Table 1. The improved precipitation over the CI region can be due

Table 2 Various statistics (mean, spatial correlation coefficient (CC), root mean square error (RMSE), and standard deviation) are calculated based on observed and model forecasted rainfall over central Indian region for different lead times

	Lead day	Mean (mm/day)	CC	RMSE (mm/day)	Standard Deviation (mm/day)
IMD-GPM		8.3			11.6
CTRL	Day-1	9.9	0.38	17.8	9.4
EXPT	Day-1	8.0	0.51	16.9	8.5
CTRL	Day-3	9.9	0.29	19.5	10.1
EXPT	Day-3	7.9	0.33	20.2	10.3
CTRL	Day-5	10.4	0.17	20.2	9.9
EXPT	Day-5	9.2	0.34	21.6	11.2
CTRL	Day-8	11.5	0.10	21.5	10.9
EXPT	Day-8	10.0	0.39	23.3	12.8

to better convective and large-scale precipitation caused by different responses of the dynamical and thermodynamical processes in the EXPT forecast (shown in a later section). On the other hand, excess rainfall over northeast India and
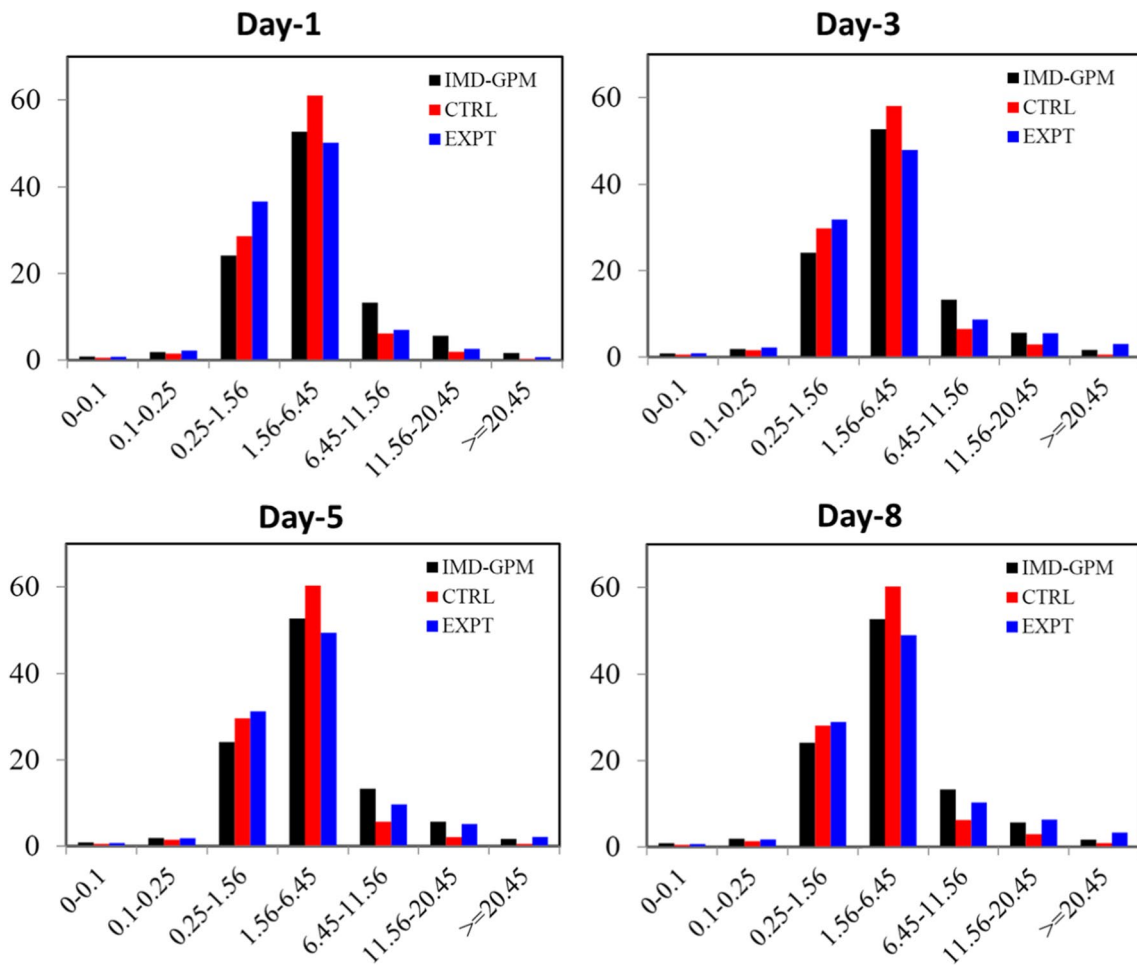
Fig.3 The rainfall PDF (%) vs. rain rate (cm day^{-1}) categories during JJAS of the year 2020 over the central Indian landmass region for different lead times derived from CTRL and EXPT forecast and compared with IMD-GPM merged gridded data
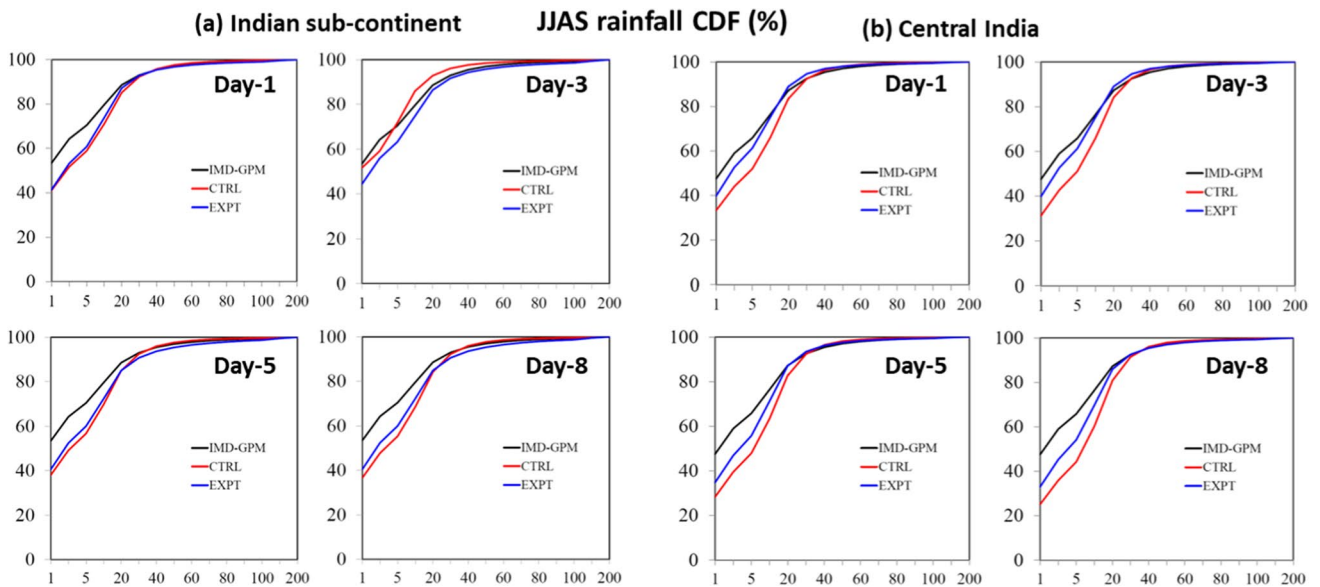

Fig.4 The rainfall CDF (%) vs. rain rate (mm day^{-1}) during JJAS of the year 2020 over the (**a**) Indian subcontinent and over the (**b**) central Indian landmass region for different lead times derived from CTRL and EXPT forecast and compared with IMD-GPM merged gridded data

the Himalayan foothills in EXPT needs a detailed investigation, which will be attempted in a future study. However, preliminary analysis indicates increased moisture convergence aided by enhanced vertical velocity in the atmospheric column over the region (Figure shown later) possibly lead to excess rainfall. Further, the above results possibly indicate that increasing the vertical resolution alone may not sufficient to improve the precipitation forecast over the Indian subcontinent region. Additional tuning of the model physics such as gravity wave drag, radiation effect of ozone may be necessary as the model top is upraised and are kept for future study.

The precipitation improvement over the core monsoon zone, i.e., CI in EXPT, is further demonstrated through the probability distribution function (PDF) as depicted in Fig. 3. The different rain rate categories are taken according to Mukhopadhyay et al. (2019) and Ganai et al. (2021). The precipitation PDF distribution suggests overestimation of lighter category rainfall (2.5–15.6 mmday^{-1}) in both CTRL and EXPT forecast for all the lead time during JJAS of the year 2020 (Fig. 3). Moreover, the overestimation of lighter

category rainfall is more in EXPT than CTRL forecast for all the lead time. The overestimation of lighter category rainfall in operational GFS is also reported in earlier studies (Mukhopadhyay et al. 2019; Ganai et al. 2021). Further, CTRL shows overestimation of moderate rainfall (15.6–64.4 mmday^{-1}) and underestimation of heavier category (> 64.5 mmday^{-1}) rainfall as compared to observation. On contrary, the EXPT forecast shows relative improvement in capturing moderate (1.56–6.45 cm day^{-1}) and heavier category (> 6.45 cm day^{-1}) rainfall for all the lead time over the CI region compared to CTRL run. The above finding reveals that the excess contribution of lighter and moderate category rainfall mainly contributes to precipitation overestimation in CTRL. Hence, it indicates that the increased vertical resolution in GFS has the potential to improve the moderate to heavier category rainfall forecast over the CI region. In order to gain further insight about the precipitation distribution, the cumulative distribution function (CDF) of 24-h accumulated precipitation is carried out over Indian subcontinent (Fig. 4a) and over CI (Fig. 4b) region. It is evident that the CDF shows marginal improvement in the lighter to moderate
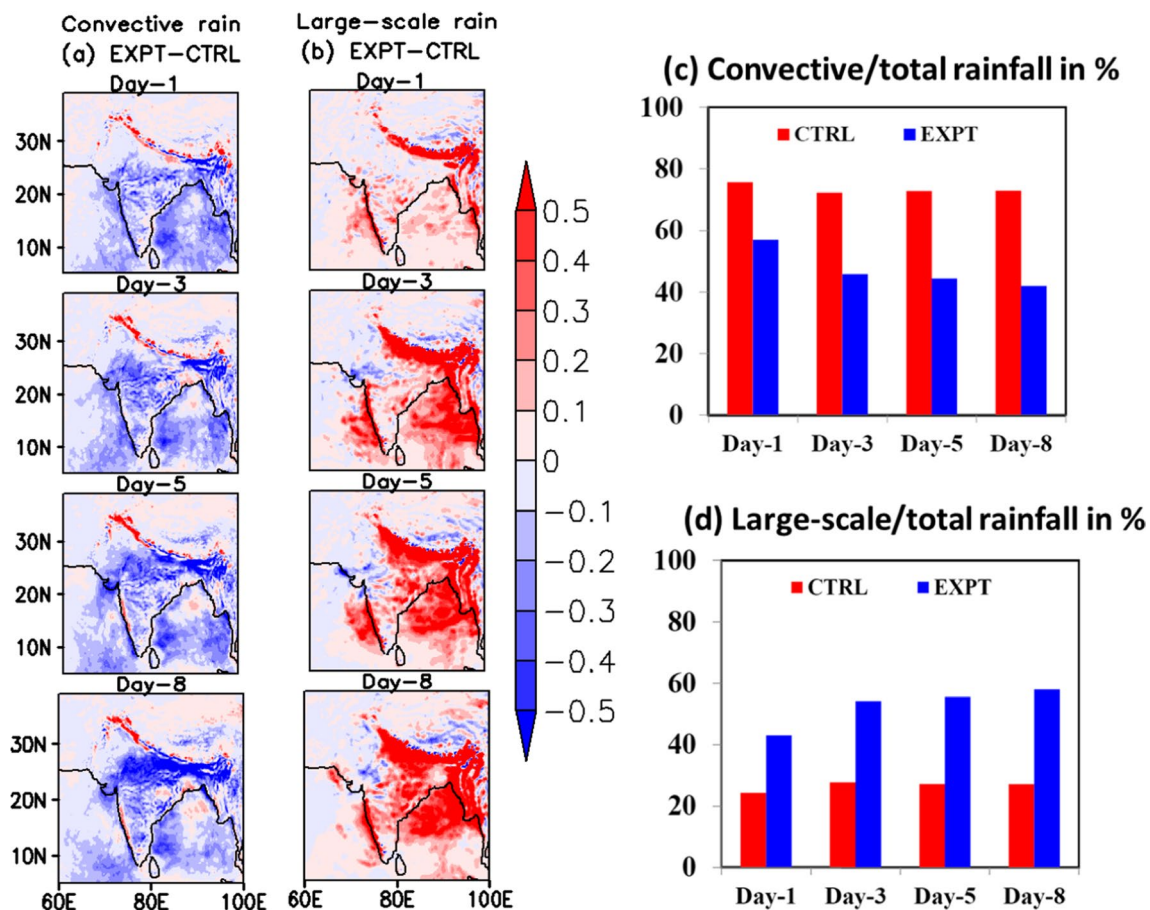

Fig.5 Spatial distribution of (**a**) convective rainfall (cm day^{-1}) and (**b**) large-scale rainfall (cm day^{-1}) in EXPT with respect to CTRL for different lead times. (**c**) and (**d**) denote convective and large-scale rain fraction over the continental Indian region for various lead days, respectively

category rainfall in EXPT forecast as compared to CTRL for all the lead time over Indian subcontinent. Further, the improvement is more prominent in EXPT over the CI region as shown in Fig. 4b. Therefore, both PDF and CDF analyses reveal that EXPT performs relatively better in forecasting lighter to heavier category rainfall over Indian region compared to CTRL forecast. It is likely that the enhanced vertical resolution allows better representation of atmospheric processes, including vertical variations in temperature, humidity, and wind. This finer representation can capture small-scale features and variations in the atmosphere that might be missed with coarser vertical resolution.

The total precipitation and its PDF and CDF show relative improvement in EXPT as compared to CTRL forecast over CI region as noted from the above analysis. However, the precipitation over Indian summer monsoon domain remains

similar or degrades over certain regions in EXPT forecast as shown in Fig. 2 and Table 1. It would be interesting to look whether the total precipitation distribution is contributed by reasonable convective and large-scale rainfall proportion. With this idea, the difference between EXPT and CTRL in forecasting convective and large-scale precipitation is shown for different lead times during JJAS of the year 2020 (Fig. 5). The computation of large-scale rainfall is similar to Ganai et al. (2021) where the convective rainfall is subtracted from the total rainfall to get the large-scale precipitation in both models. It is worth mentioning that Sabeerali et al. (2015) showed 55% (45%) contribution to total rainfall is contributed by convective (large-scale) rainfall based on TRMM 3A25 observation over the ISM region. Further, Pokhrel and Sikka (2012) brought out the convective and large-scale precipitation distribution based on observation (TRMM 3A25)
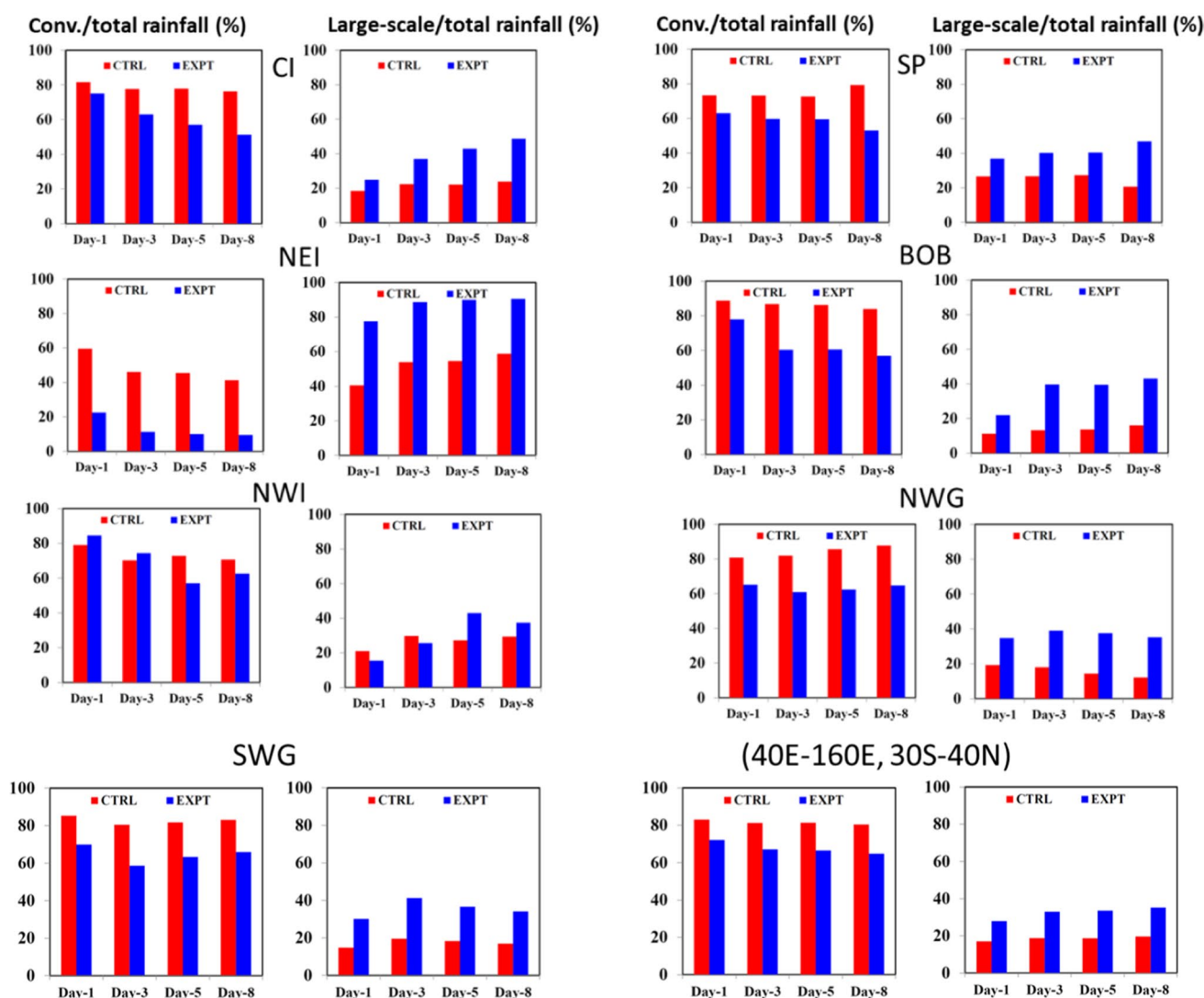

Fig.6 The convective and large-scale rainfall fraction (%) over the different regions of India (as in Fig. 1) from CTRL and EXPT forecast for Day-1, Day-3, Day-5 and Day-8 lead times over India

during 1998–2010 over different parts of Indian region. As per their (Table 2 in their paper) study, majority of the region receives (50–55%) convective and (45–50%) large-scale rainfall except northeast India where the contribution of large-scale rainfall (52%) is more than convective (48%) rainfall. The spatial distribution indicates that the convective (large-scale) rainfall is decreased (increased) over the majority of the Indian landmass regions in the EXPT forecast as compared to the CTRL forecast for all the lead times (Fig. 5a and b). In addition, the large-scale rainfall over the northeast India, the Himalayan foothills, WG, BoB region is considerably more in EXPT as compared to CTRL forecast (Fig. 5b). Furthermore, the convective rainfall is enhanced over WG region in EXPT compared to CTRL forecast for Day-5 and Day-8 lead time. It is likely that the excess total

rainfall in EXPT (Fig. 2c and d) as compared to CTRL forecast is contributed mainly by the large-scale precipitation. It is likely that the higher vertical resolution lead to enhance large-scale vertical moisture convergence associated with strong vertical ascending motion resulted in enhanced large-scale precipitation over the region (Figure shown later). A similar decrease (increase) in convective (large-scale) precipitation is noted in the higher vertical resolution model by Lee et al. (2019). They showed that enhanced surface flux and vertical transport of moisture in the higher vertical resolution model led to increased large-scale precipitation. The above findings are further established by the convective (large-scale) precipitation fraction over the Indian subcontinent region as depicted in Fig. 5c and d. The CTRL forecast exhibits around 70–75% convective and 25–30% large-scale
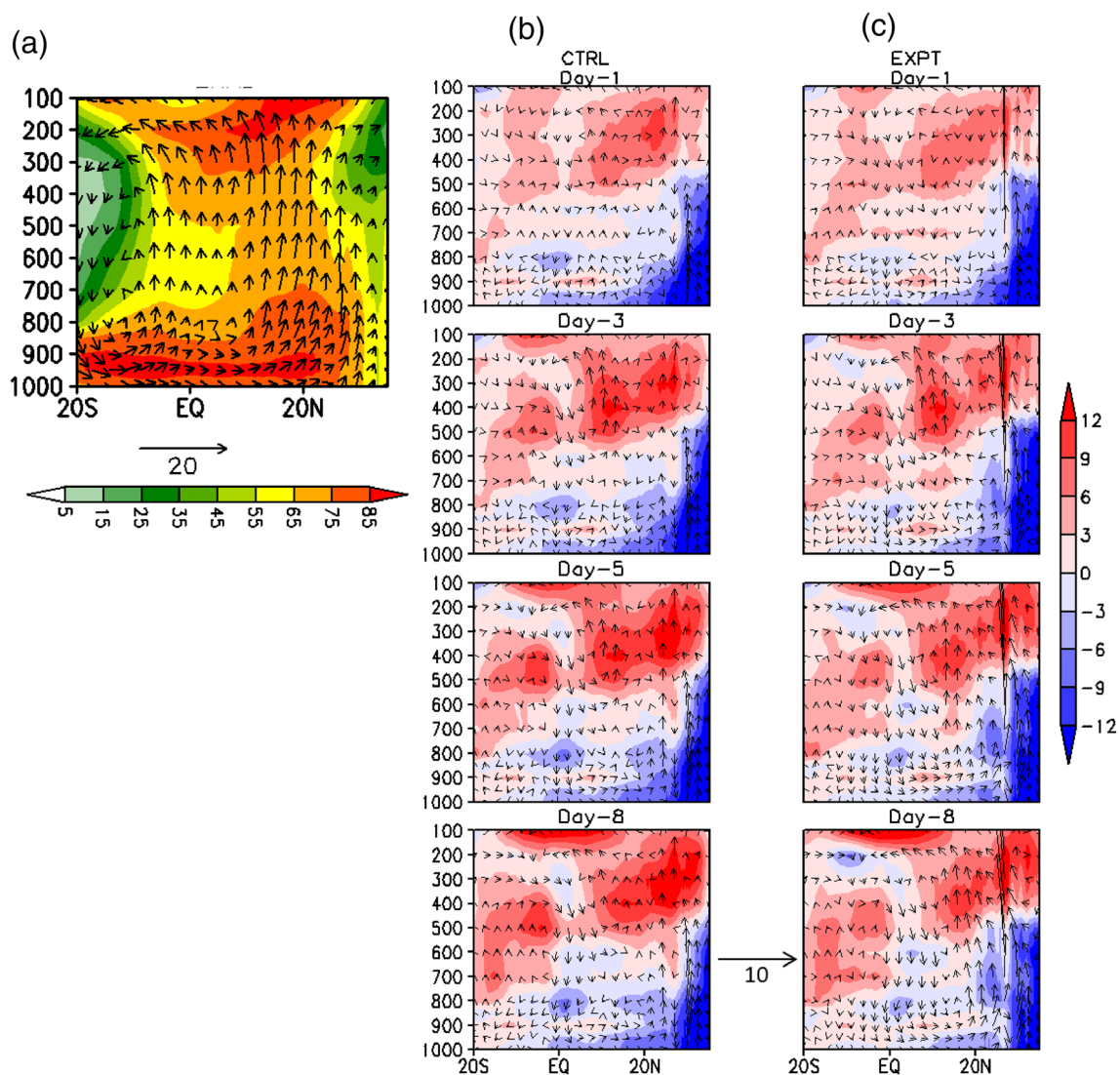

Fig.7 Latitude-pressure plot of mean regional Hadley cell circulation (vector, v-wind vs. (-1) *omega×100) and RH (shaded in %) distribution averaged over 65°E-95°E during JJAS of 2020 from (**a**) ERA5. The bias in Hadley cell circulation (vector) and RH (shaded) in (**b**) CTRL, and (**c**) EXPT forecast with respect to ERA5 at different lead times, respectively

rainfall for all the lead times (Fig. 5c). On the other hand, for EXPT, it is around 50–60% convective and 40–50% large-scale rainfall. Further, the convective and large-scale rainfall distribution is shown in Fig. 6 over different regions over India as per Fig. 1 from both CTRL and EXPT and compared with Pokhrel and Sikka (2012). It is noted from Fig. 6 that EXPT shows enhanced contribution of large-scale rainfall compared to CTRL forecast for all the lead times over majority the regions over India. However, over the northeast India region, model appears to considerably overestimate the contribution of large-scale rainfall compared to observation. Therefore, the above sensitivity study results show that enhanced total rainfall (Table 1) over Indian landmass region is mostly contributed by the increased large-scale rainfall over northeast India, Himalayan foothills and WG regions. On the other hand, relatively improved total precipitation distribution over CI region (Table 2) is due to reasonable contribution of convective and large-scale rainfall in EXPT.

3.2 Wind circulation, dynamical and thermodynamical processes

The sensitivity of increased vertical resolution in GFS on forecasting large-scale circulation and dynamics are analyzed in the present section. The vertical profile of relative humidity and circulation (meridional-vertical), the regional Hadley cell (averaged over 65°E-95°E) is shown for ERA5 and both models forecast for different lead times (Fig. 7). Observation based on ERA5 reanalysis shows moist lower troposphere (relative humidity (RH) > 75%) within the surface to 850 hPa level over 20°S-25°N domain (Fig. 7a). Associated with

moist planetary boundary layer, the low-level wind converges over Indian mainland region (10°N-25°N), and ascends over higher altitude. Subsequently, the strong ascending branch diverges in the upper level and descends over the Indian Ocean region. The moist atmospheric column (RH > 65%) is also associated with strong ascending motion over the Indian mainland region. Both CTRL and EXPT is able to forecast the above circulation and moisture distribution reasonably for all the lead time, as shown in Fig. 7b and c, respectively. However, detailed analysis indicates that both the models slightly underestimate the lower-level moisture and overestimate the mid and higher-level moisture distribution compared to ERA5. This is likely influenced the vertical heating distribution through phase changes and leads to marginally weaker low-level wind circulation and stronger mid to higher-level ascending motion in both models (Fig. 7b and c). However, closer bias analyses suggests relatively improved lower and middle level moisture distribution in EXPT (Fig. 7c) forecast compared to CTRL run (Fig. 7b) for all the lead times. The enhanced vertical resolution in the EXPT set-up leads to the reasonably resolved vertical moisture distribution compared to the CTRL model. This is also consistent with the study by Lee et al. (2019), which documented better tropospheric moisture distribution in higher vertical resolution version of the Korean operational medium range forecast model.

To assess the processes responsible for relatively better model forecast over the CI region with enhanced vertical resolution in GFS, various dynamical and thermodynamical processes are investigated during JJAS of the year 2020, as shown in Fig. 8. The lower-level moisture convergence is overestimated in both CTRL and EXPT as compared to
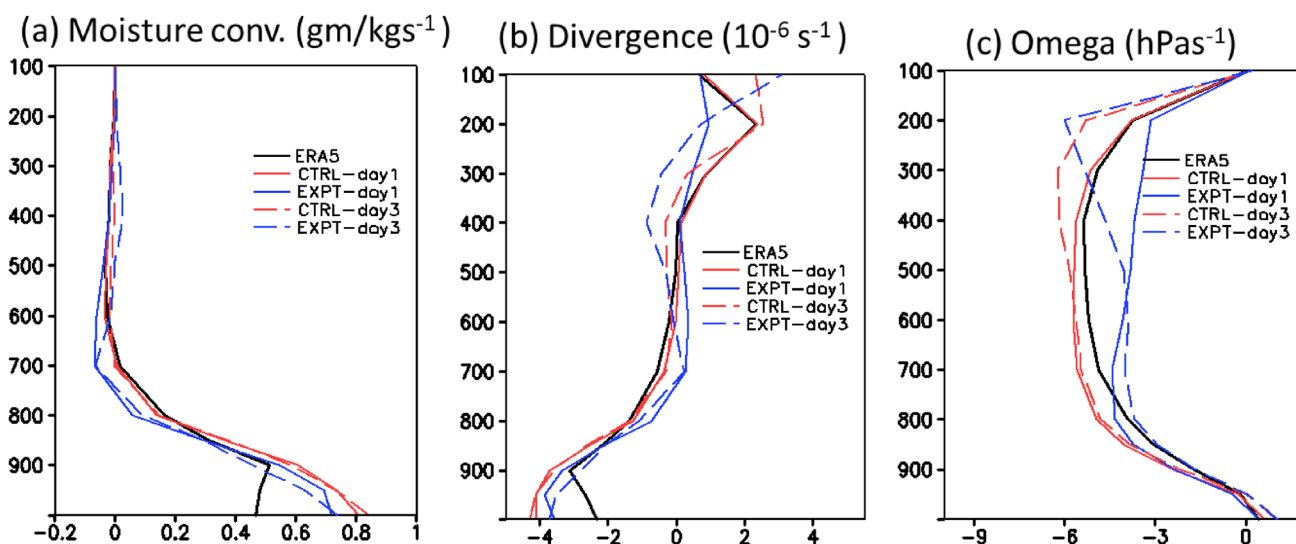

Fig.8 JJAS mean vertical profiles of (**a**) moisture convergence (gm/kgs⁻¹), (**b**) divergence (10⁻⁶ s⁻¹), and (**c**) vertical velocity (hPas⁻¹) for ERA5 (black line), CTRL (red line) and EXPT (blue line) for day-1 and day-3 lead time over the central Indian landmass (73°E-85°E, 18°N-27°N) region

ERA5 reanalysis (Fig. 8a). However, the EXPT forecast shows relative improvement in the lower level over CTRL for day-1 and day-3 lead time. On contrary, the middle level moisture convergence is underestimated in the sensitivity experiment. The larger moisture convergence in the lower level is consistent with enhanced low-level convergence in both models (Fig. 8b). Compared to CTRL, the increased vertical resolution in EXPT shows better lower-tropospheric moisture distribution (Fig. 8a and b) and associated moisture convergence over the CI region. The moisture distribution in the tropospheric column is mainly driven by vertical atmospheric circulation. The vertical velocity in the atmospheric column indicates that both models show reasonable lower-level vertical motion (Fig. 8c). However, EXPT suggests underestimation in the strength of the vertical velocity between 700-200 hPa for both Day-1 and Day-3 lead time.

It is found that the mid-level vertical velocity (Fig. 8c) and associated moisture convergence (Fig. 8a) is underestimated in EXPT forecast and needs to be addressed with further investigation. However, it is noted that the increased vertical resolution in EXPT has reasonable lower tropospheric vertical motion with slightly improved lower level moisture convergence.

The relative improvement in the precipitation distribution and associated underlying dynamical processes over the CI region in the sensitivity experiment is noted from the previous results. However, one of the major drawbacks of the present study is to having considerable overestimation of precipitation over the Himalayan foothills, northeast India, and WGs region in the EXPT forecast. This excess rainfall eventually contributes to the increased rainfall amount over the Indian landmass region as shown in Table 1. To gain

Fig.9 JJAS mean vertical profiles of (**a**) moisture convergence (gm/kgs^{-1}), (**b**) divergence (10^{-6} s^{-1}), (**c**) vertical velocity (hPas^{-1}), and (**d**) apparent heat source (Q1) for ERA5 (black line), CTRL (red line) and EXPT (blue line) for day-1 and day-3 lead time over the Himalayan foothills and northeast India (84°E-96°E, 26°N-28°N) region
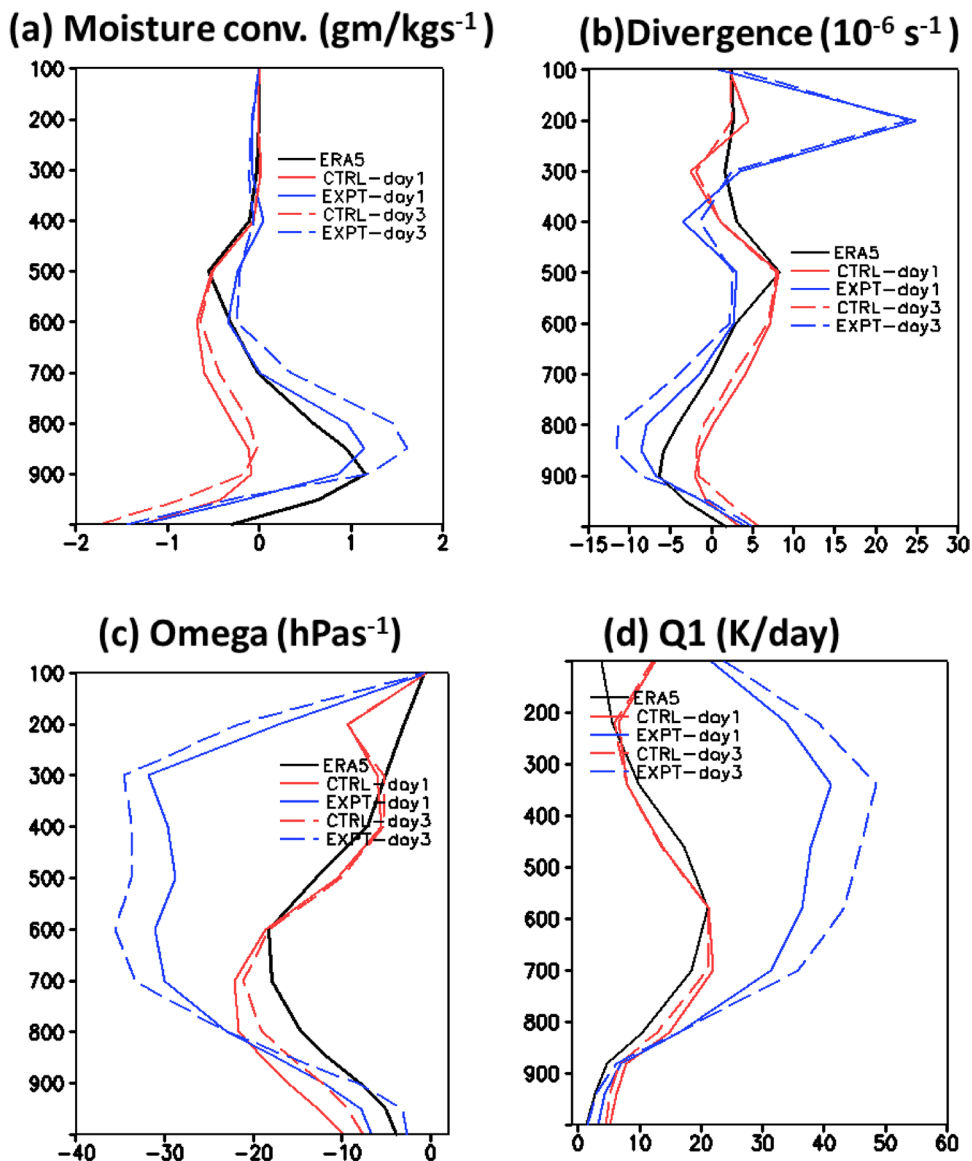
insight about the dynamical and thermodynamical processes responsible for the excess rainfall over the Himalayan foothills and northeast India region (26ºN-28ºN, 84ºE-96ºE), various parameters are shown in Fig. 9 for both models and observation. The moisture convergence (Fig. 9a) indicates stronger convergence than ERA5 in EXPT forecast between 900–400 hPa level for both Day-1 and Day-3 lead times. On contrary, CTRL appears to considerably underestimate the moisture convergence from surface to 500 hPa level. The stronger moisture convergence in the lower to upper level in EXPT is associated with enhanced wind convergence (Fig. 9b) in low level and divergence in the upper level. Consistent with the above findings, the vertical velocity also shows considerably strong ascending motion throughout the troposphere in the sensitivity experiment (Fig. 9c). On the other hand, CTRL has stronger low level ascending motion and reasonable vertical motion in the middle to upper troposphere compared to ERA5. The Himalayan foothills

and northeast India region showed excess contribution of large-scale precipitation (Fig. 9b) to the total rainfall. It will be worth to evaluate the large-scale heating distribution following Yanai et al. (1973) over the region. The large-scale apparent heat source (Q1) indicates much stronger heating throughout the troposphere in EXPT compared to ERA5 indicating intense convection over the region (Fig. 9d). On the other hand, CTRL predicts reasonable heating throughout the troposphere. The above analysis brings out the reason behind the excess rainfall over the Himalayan foothills and northeast India region in EXPT forecast. It is likely that the strong vertical motion resulted from excess moisture convergence leading to enhanced moisture detrainment from the upper level, which in turn increases the large-scale rainfall and associated large-scale heating over the region. All these processes lead to precipitation overestimation over the region in EXPT forecast. Further, it is likely that the similar processes responsible for the excess rainfall over the
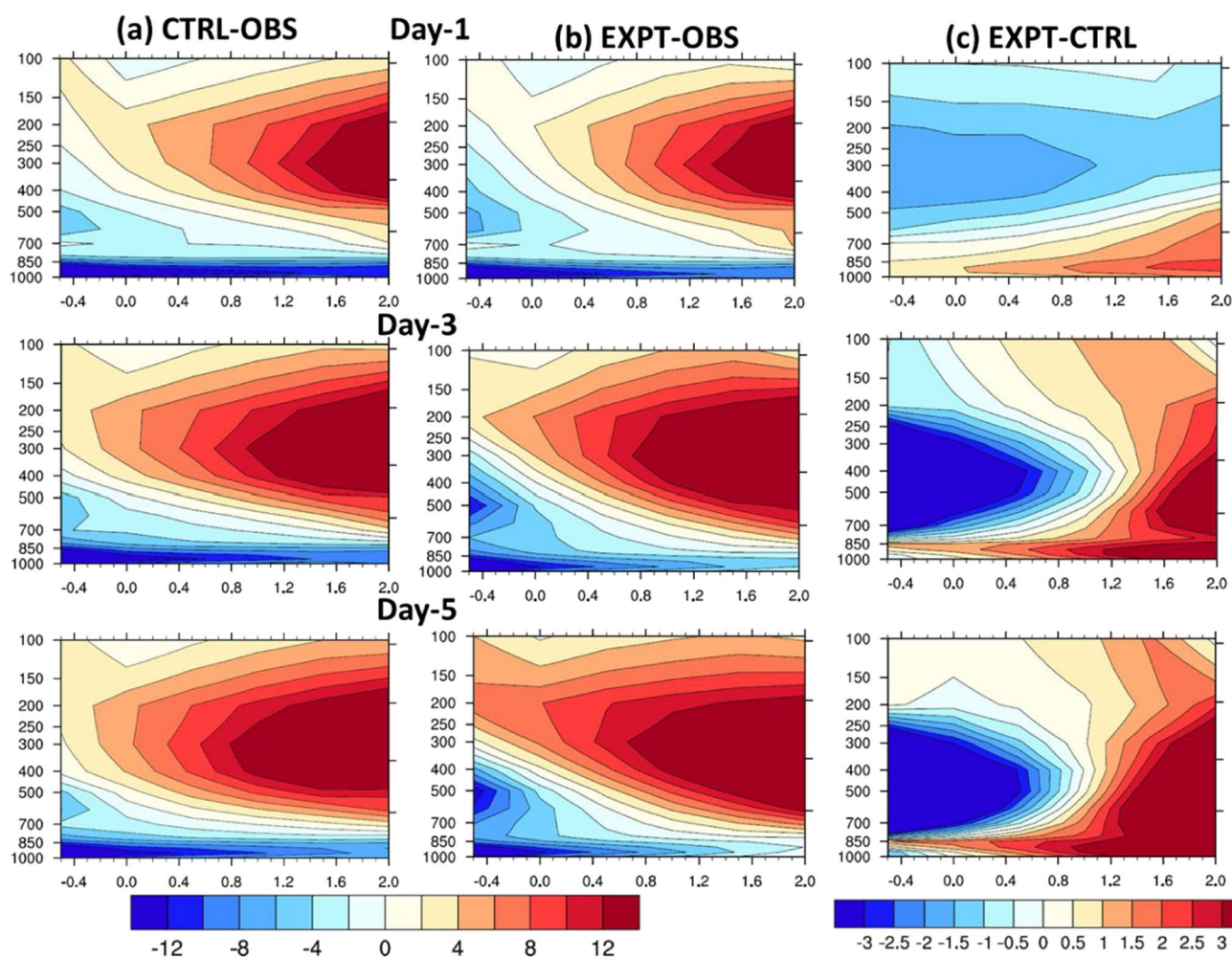

Fig.10 Vertical profile of bias in relative humidity (shaded in %, along the y-axis) as a function of rain rate (mm day^{-1}, along the x-axis) in (**a**) CTRL, (**b**) EXPT with respect to observation (ERA5 vs. IMD-GPM merged data), and (**c**) EXPT with respect to CTRL over the central Indian landmass region during JJAS of 2020 for different lead times

WGs region (Figure not shown). The above analysis suggests that further improvement in the model physics is needed to address the above issues.

To gain more insight into the impact of enhanced vertical resolution in the rainfall and moist convective processes, the vertical distribution of relative humidity as a function of rain rate is plotted in Fig. 10 during JJAS of the year 2020 over the CI region. The bias analysis demonstrates that both CTRL and EXPT show a systematic underestimation in the lower-level (below 850 hPa) moisture over the CI region (Fig. 10a and b). In addition, they also show an overestimation of moisture in the mid to upper troposphere for moderate to heavier category rainfall. Mukhopadhyay et al. (2019) and Ganai et al. (2021) reported similar underestimation of lower-level moisture and overestimation of mid to upper-tropospheric moisture in CTRL forecast. Detailed analyses further reveal that relatively the lower level biases are improved in EXPT than CTRL forecast as indicated in Fig. 10c. Bhaskar Rao et al. (2010) showed increased vertical resolution in the lower

troposphere produces better moisture distribution which helps in efficient intensification for tropical cyclone. The lower-tropospheric humidity plays a vital role in preconditioning the atmosphere for further triggering, sustaining and growth of convection. Higher vertical resolution helps in representing the boundary layer more accurately, capturing the interactions between the surface and the atmosphere. Better lower tropospheric moistening due to reasonable moisture convergence in EXPT helps improve moist-convective feedback in the atmosphere. Therefore, the enhanced vertical resolution in EXPT helped capture better dynamical and thermodynamical processes in the atmosphere (Fig. 8), eventually leading to better precipitation distribution over the CI landmass region.

3.3 Skill scores analysis

The above analyses demonstrate the fidelity of the EXPT model in forecasting various aspects of the monsoon features during JJAS of the year 2020. Further to demonstrate

Fig.11 Evaluation scores of CTRL (red line) and EXPT (blue line) for 3 h accumulated precipitation forecasts over Indian subcontinent (solid line) and over central India (dashed line) at different lead hours: (**a**) RMSE (mmhr^{-1}), (**b**) bias (mmhr^{-1}), and (**c**) correlation coefficient
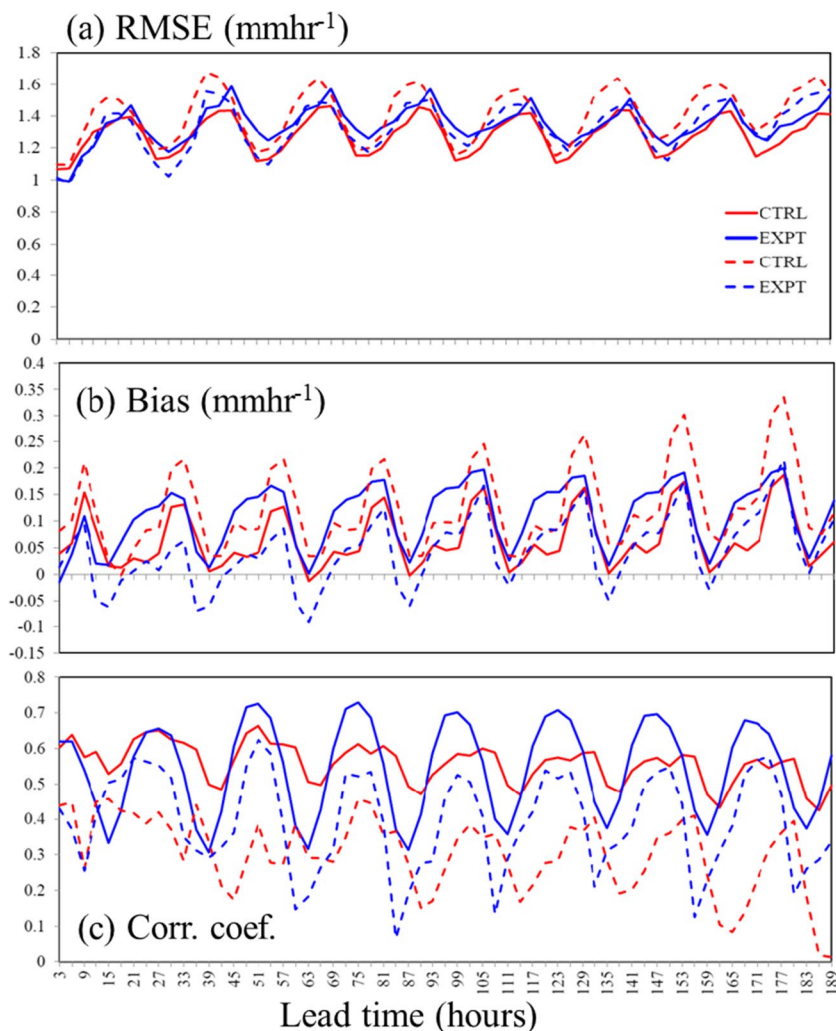
the model skill, the evaluation scores based on precipitation forecast are carried out in Fig. 11. The RMSE, bias and correlation coefficient (CC) are calculated for both models with respect to observation. It is noted that the RMSE, bias and CC are relatively better in CTRL than EXPT over the Indian subcontinent region. On contrary, EXPT shows better skills over the CI region as depicted in Fig. 11. Additionally, to investigate the forecast skill of EXPT objectively, Bias score (B) and Equitable Threat Score (ETS) are computed over the Indian subcontinent and CI landmass region. These scores are calculated based on a contingency table (Wilks 2011) and are similar to Ganai et al. (2021). The Bias score is demonstrated in Fig. 12 over the Indian subcontinent (Fig. 12a-c) and CI landmass region (Fig. 12d-f) for day-1, day-2, and day-3 lead times. A Bias score of 1 suggests a perfect forecast, greater than 1 indicates overforecasting, and less than 1 represents under-forecasting. Over the Indian subcontinent, EXPT shows a relatively better bias score for 2 cm day^{-1} and 5 cm day^{-1} precipitation thresholds than CTRL forecast for all the lead times (Fig. 12a-c). However, for higher thresholds, EXPT shows overforecasting for all the lead times. This may be due to the tendency of EXPT to overforecast the frequency of heavier rainfall, mainly over the northeast and

Himalayan foothills regions, as noted in Fig. 2c. It is further established in the Bias score over CI landmass region (Fig. 12d-f) in EXPT forecast. Here, it is evident that EXPT shows better Bias score for all precipitation thresholds for all the lead times as compared to CTRL forecast. This result is consistent with the fact that total precipitation distribution is improved over the CI region in the EXPT forecast, as shown in Fig. 2c. Further, the ETS is demonstrated in Fig. 13 over the Indian subcontinent and CI region, a score of 1 indicates perfect forecast. This metric takes into consideration the correct forecast obtained due to chance and informs how the forecast 'yes' events fared against the observed 'yes' events. Similar to the Bias score, ETS is marginally better in CTRL than EXPT over the Indian subcontinent region for all the lead time (Fig. 13a-c). However, EXPT performs better than CTRL over the CI region for all the lead times. The above analyses indicate better forecast skill in EXPT than CTRL forecast over the CI region. However, over the whole Indian landmass region, the forecast skill degrades in EXPT compared to CTRL forecast. The relatively better forecast skill in EXPT is likely due to enhanced vertical resolution, which resolves the processes in the tropospheric column and subsequently improves the precipitation distribution.
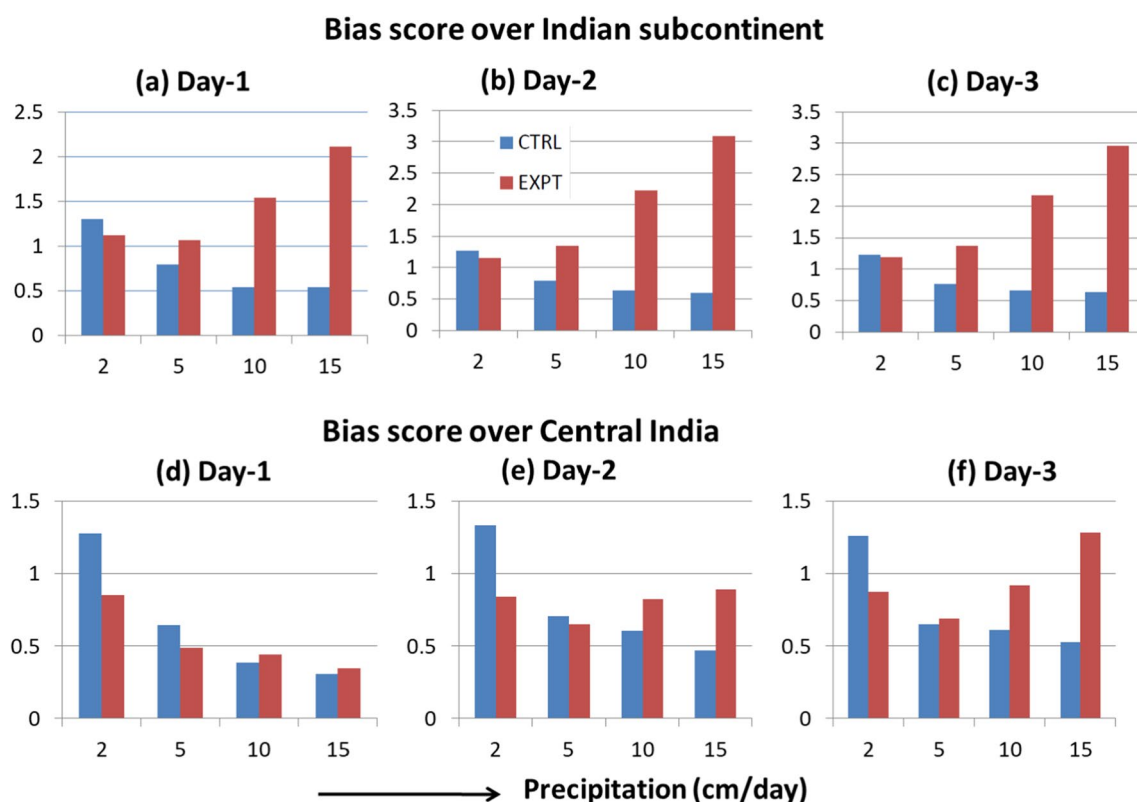

Fig.12 (**a-c**) represent Bias score for CTRL (blue bar) and EXPT (red bar) for day-1 to day-3 lead days respectively over the continental Indian region during JJAS of 2020. (**d-f**) represent similar analysis but over central India region. X-axis represents various precipitation thresholds (cm day^{-1})

3.4 Diurnal cycle of precipitation and extreme rainfall case study

It is well known that the diurnal cycle of solar radiation plays a major impact on the local and regional variability of the earth's weather, particularly on tropical storms and associated winds and precipitation. All the above analyses demonstrate the performance of EXPT in forecasting the Indian summer monsoon features in daily to seasonal scale during JJAS of the year 2020. In addition to the daily to seasonal scale, the diurnal precipitation cycle is also investigated in the present section. Previous studies (Yang and Slingo 2001; Dai and Trenberth 2004; Ganai et al. 2016; Mukhopadhyay et al. 2019) have highlighted the diurnal cycles in convection, cloudiness and circulation and their distributions are a good test bed for the validation of weather and climate models. The JJAS mean precipitation bias spatial distribution is shown in Fig. 14 for 0230 Indian standard time (IST) to 2330 IST at 3 hourly intervals for day-1 lead time for both CTRL and EXPT forecast. The CTRL forecast indicates precipitation overestimation over CI and adjacent landmass region, northeast India and the Himalayan foothills region (Fig. 14a) for all the times. The above overestimation

appears to increase as we move from morning to afternoon hours in the CTRL forecast. On the contrary, the EXPT forecast shows relative improvement in forecasting the above biases over the ISM region for all the times (Fig. 14b). The precipitation overestimation reduces in EXPT over CI and adjacent landmass region compared to CTRL forecast. However, the precipitation is grossly overestimated over the Himalayan foothills and northeast India region for all the times (except 0830 IST) (Fig. 14b). Additionally, the precipitation overestimation is noted over WGs region for majority of the time of the day in EXPT forecast. These diurnal biases are eventually added up in the daily to seasonal scale over the above region and showed precipitation overestimation as shown in Fig. 1c. On contrary, the improvement over CI region is further established from the area averaged mean bias and spatial correlation coefficient (CC) statistics which are mentioned at the top of each plot (Fig. 14a and b). Similar improved spatial diurnal precipitation distribution over the CI region is also noted for day-3 lead time (Figure not shown). Overall, it is found that the consistent with the daily to seasonal scale, diurnal scale precipitation also shows relative improvement over the CI landmass region in EXPT sensitivity forecast compared to CTRL. However, the issue
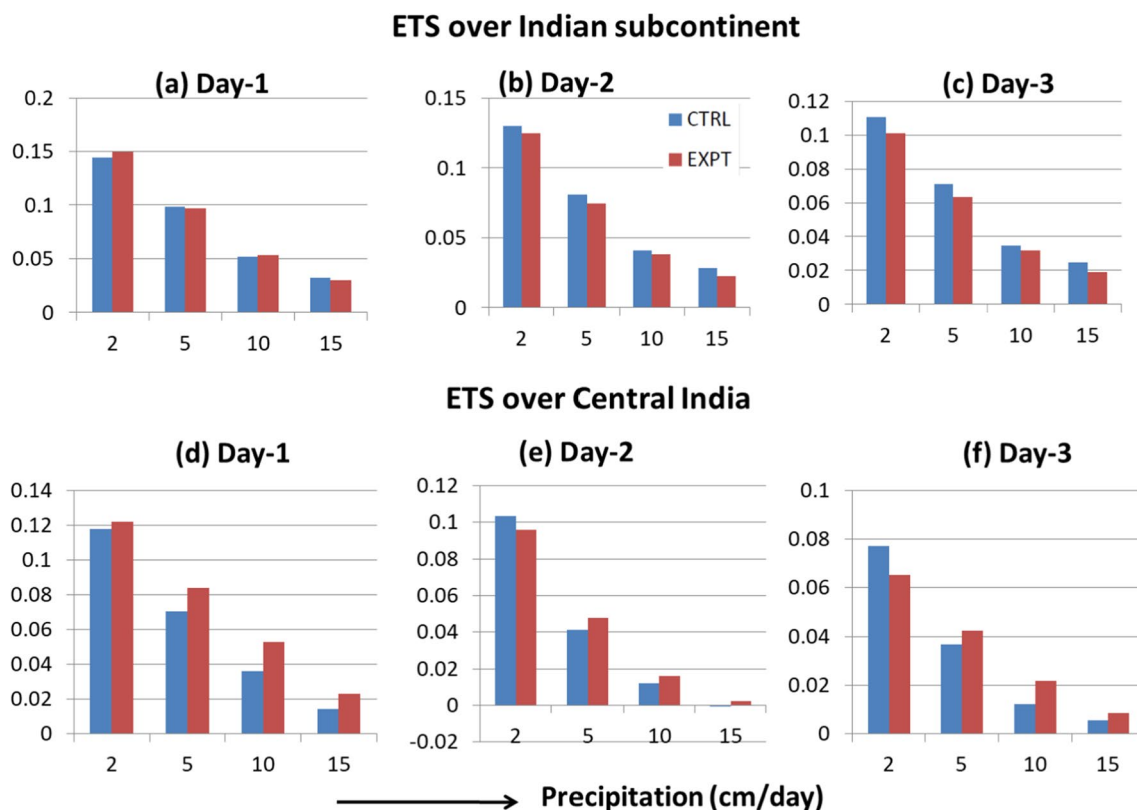

Fig.13 (**a-c**) represent ETS score for CTRL (blue bar) and EXPT (red bar) for day-1 to day-3 lead days respectively over the continental Indian region during JJAS of 2020. (**d-f**) represent similar analysis but over central India region. X-axis represents various precipitation thresholds (cm day^{-1})

of precipitation overestimation over the Himalayan foothills, northeast India, and WGs region is also prominent in the diurnal scale which needs to be further addressed.

Further, the diurnal cycle of precipitation is investigated over different parts of the Indian region, as shown in Fig. 1. These regions are chosen based on their distinct local features, which will be discussed later in this section. The above boxes are similar to Mukhopadhyay et al. (2019) (Fig. 12 in their paper). The diurnal cycles of precipitation are shown in Fig. 15. Over the CI region, studies (Sahany et al. 2010; Ganai et al. 2016) showed that the observed afternoon/early evening peak over the CI landmass region is primarily due to the thermodynamic response to the surface solar heating. However, CTRL shows the peak rainfall 3 h earlier than observation, and the precipitation amplitude is also considerably overestimated. Similar results were also demonstrated by Mukhopadhyay et al. (2019) in the CTRL forecast. On the contrary, EXPT shows a better diurnal cycle of precipitation over the CI region. It is able to capture the magnitude and phase reasonably better as compared to CTRL forecast over the CI region. Over the BoB region, the observed diurnal precipitation cycle peaks at around

1430 IST. Yang and Slingo (2001) suggested it could be due to diurnally generated gravity waves. The CTRL forecast indicates reasonable amplitude of the diurnal cycle over the region for day-1 and day-3 lead times. On the contrary, EXPT considerably underestimates the amplitude of the diurnal precipitation for day-1 lead time and slightly overestimates for day-3 lead time. Interestingly, the diurnal phase is reasonably captured in both models for both lead times. Over northeast India, the early morning observed peak can be associated with the interaction between katabatic winds and the southwesterly winds (Sahany et al. 2010). While the CTRL forecast shows a reasonable diurnal cycle over the region, EXPT grossly overestimates the amplitude of the precipitation for both lead times. The result is consistent with the fact that EXPT overestimates the seasonal mean precipitation over northeast India, as shown in Fig. 2c. Further, over northwest India, the observed precipitation peaks at around 1730 IST and also has a secondary peak in the morning hours (0830 IST). Both models fail to capture the observed afternoon precipitation peak, showing an early morning peak for both lead times. Mukhopadhyay et al. (2019) showed a similar result in the CTRL forecast. Over
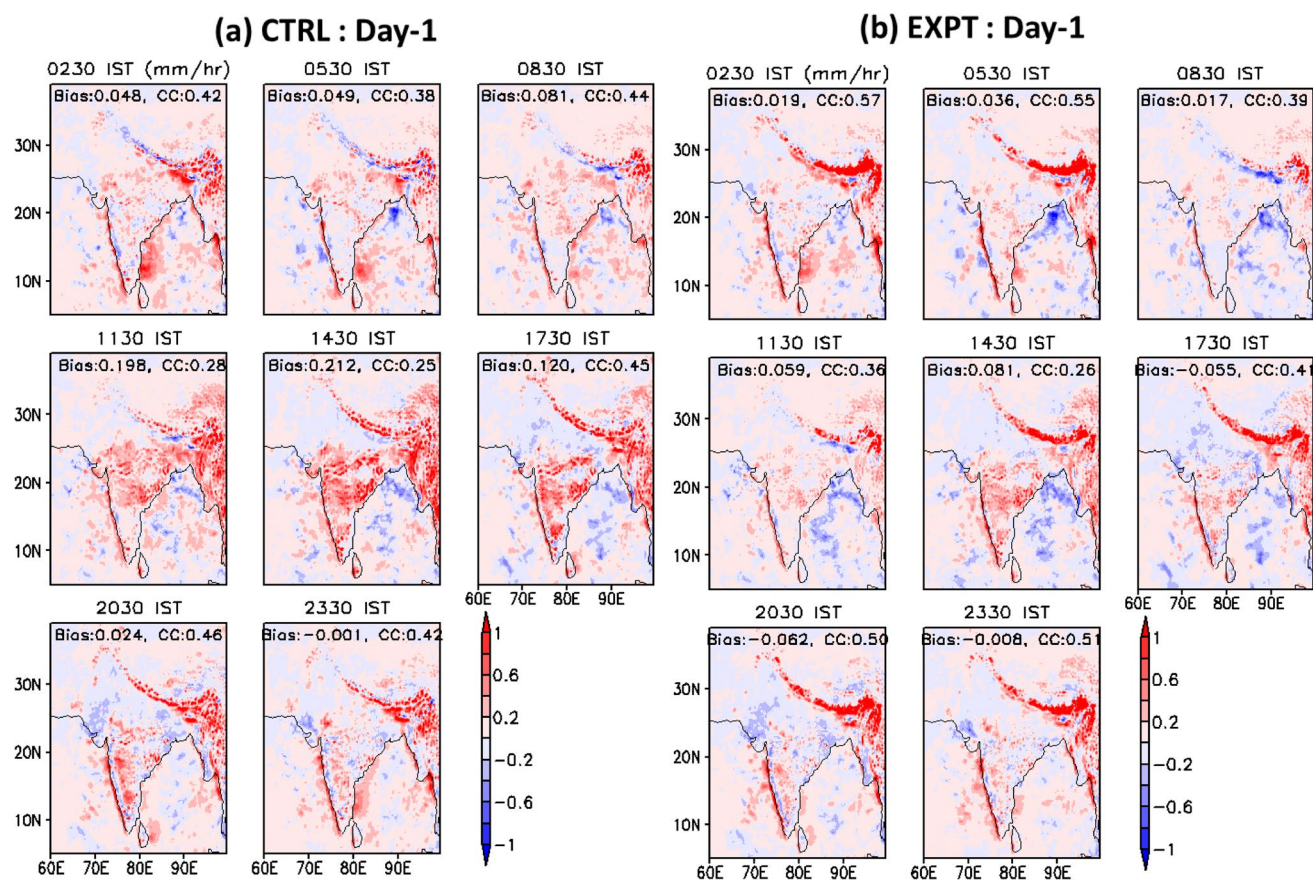

Fig. 14 The spatial distribution of precipitation bias (mm hr^{-1}) in (**a**) CTRL and (**b**) EXPT with respect to observation for day-1 lead time for 0230 IST to 2330 IST at 3 hourly intervals. The domain averaged precipitation bias and spatial correlation coefficient is mentioned in each plot

the Western Ghats (WG) regions, the observed precipitation peak is due to the interaction between the land-sea breeze and the prevailing monsoonal flow (Sahany et al. 2010). Both models report an overestimation of diurnal precipitation amplitude over northern and southern WG regions. However, EXPT captures the diurnal precipitation peak relatively better than CTRL for both lead times over the northern WG region. Over the southern peninsula and Indian Ocean region, both models show reasonable diurnal amplitude and phase for both the lead times. Over the Indian Ocean region, the diurnal cycle of precipitation may be attributed to the lifetime of large-scale convective systems and complex interaction between clouds, radiation and near-surface thermodynamics (Chen and Houze 1997; Sui et al. 1997; Sahany et al. 2010). The diurnal cycle of precipitation amplitude is underestimated more in EXPT than CTRL forecast for day-1 and day-3 lead time.

The above analyses demonstrate the role of enhanced vertical resolution in GFS in capturing the diurnal cycle of precipitation over different parts of India. Overall, it is found that EXPT has predicted the diurnal cycle relatively well over the CI landmass region than CTRL forecast. It captures the diurnal precipitation amplitude and phase over the region. However, it shows discrepancies in the diurnal cycle compared to observation over some areas (northeast and northwest India) which could be due to model's inability to represent the realistic local dynamical and thermodynamical processes (Fig. 8). It indicates further model improvement is required to address those issues.

All the above analyses documented that the GFS model with enhanced vertical resolution shows better precipitation distribution and skill mainly over CI and neighbouring regions. It is well established that the heavy (> 60 mm day^{-1}) to extreme (> 200 mm day^{-1}) precipitation events show an
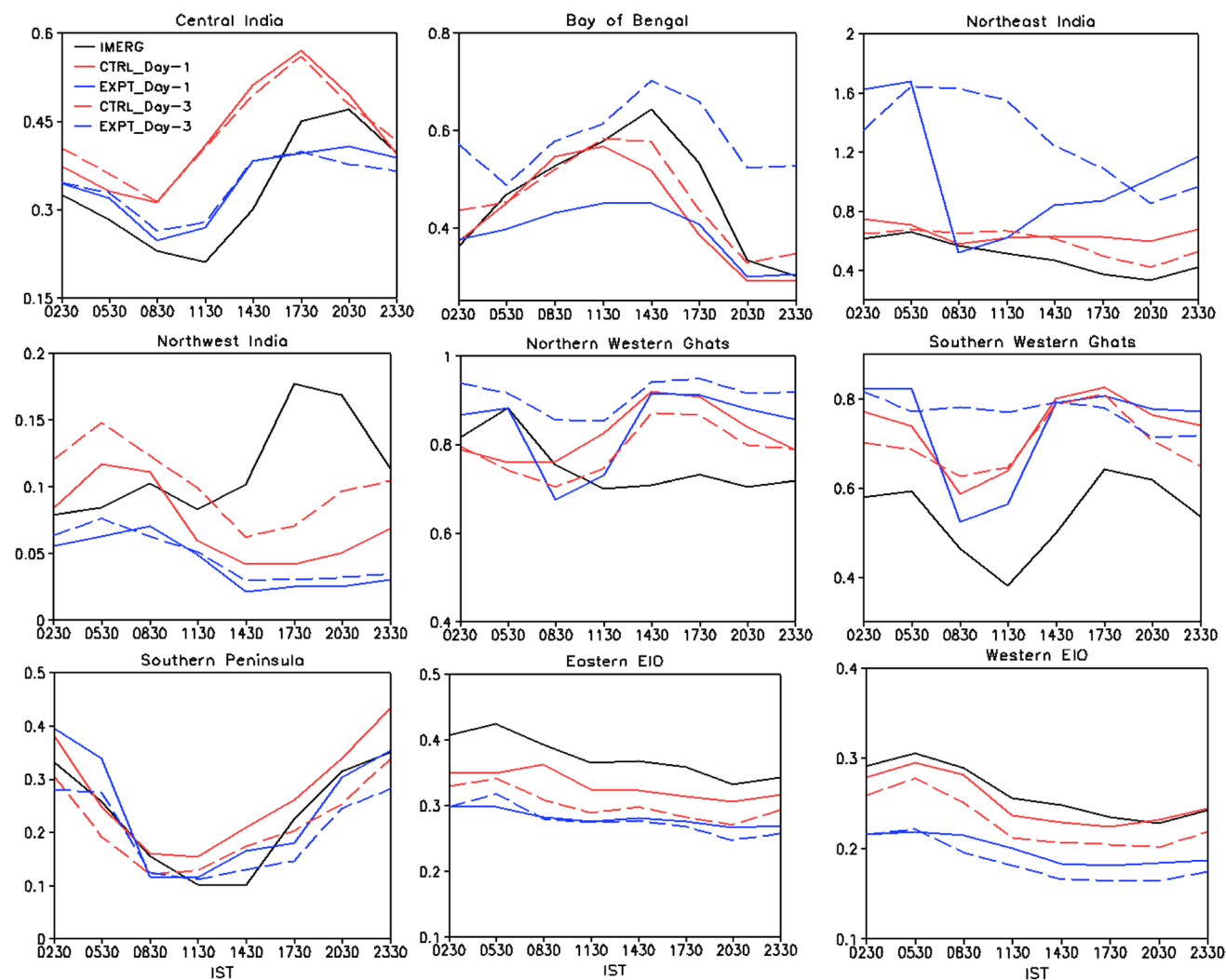

Fig.15 Diurnal cycle of precipitation (mm hr^{-1}) as obtained from IMERG (black line), CTRL (red line), and EXPT (blue line) forecast at different lead times during JJAS of 2020 over different selected regions as in Fig. 1

increasing trend over the Indian subcontinent (Goswami et al. 2006; Rajeevan et al. 2008; Roxy et al. 2017). Extreme precipitation events have a devastating socio-economic impact on the livelihood of India's vast population. Therefore, skilful prediction of heavy to extreme precipitation is crucial for the country. It is worth noting that EXPT shows better rainfall PDF for heavy to extreme rainfall category than CTRL forecast for all the lead time (Fig. 3). Therefore, it would be interesting to investigate whether the enhanced vertical resolution in the GFS model is able to better performance in predicting the intensity and location of the heavy to extreme events over the Indian subcontinent. In the present manuscript, extreme precipitation event on 4-6th August 2020 over Mumbai and the surrounding region is chosen as a forecast demonstration. Figures 16, 17, and 18 demonstrate the precipitation distribution for the 4th, 5th and 6th of August 2020 for both observation and models. During 4th to 6th August, 2020, observation

shows extreme rainfall over Mumbai and surrounding regions (Figs. 16, 17 and 18). Both models indicate heavy rain for day-1, day-2, and day-3 lead time for all the above days (4-6th August). However, both models appear to show a slight shift in the precipitation maximum pattern for the 4th and 5th of August for all the lead times (Figs. 16 and 17). However, for 6th August, both models predict the precipitation pattern reasonably well for day-1 lead time (Fig. 18). The intensity of the spatial precipitation distribution is enhanced in EXPT than CTRL forecast for all the days. It is evident in Fig. 19 (averaged over 18.5°N-19.5°N, 72.5°E-73.5°E) that EXPT shows enhanced precipitation intensity for most of the lead times for all the days (4-6th August). Overall, the above analysis indicates that EXPT tends to forecast enhanced precipitation intensity than CTRL forecast, and EXPT retains precipitation intensity for longer lead times. Although EXPT shows its potential in predicting extreme precipitation events
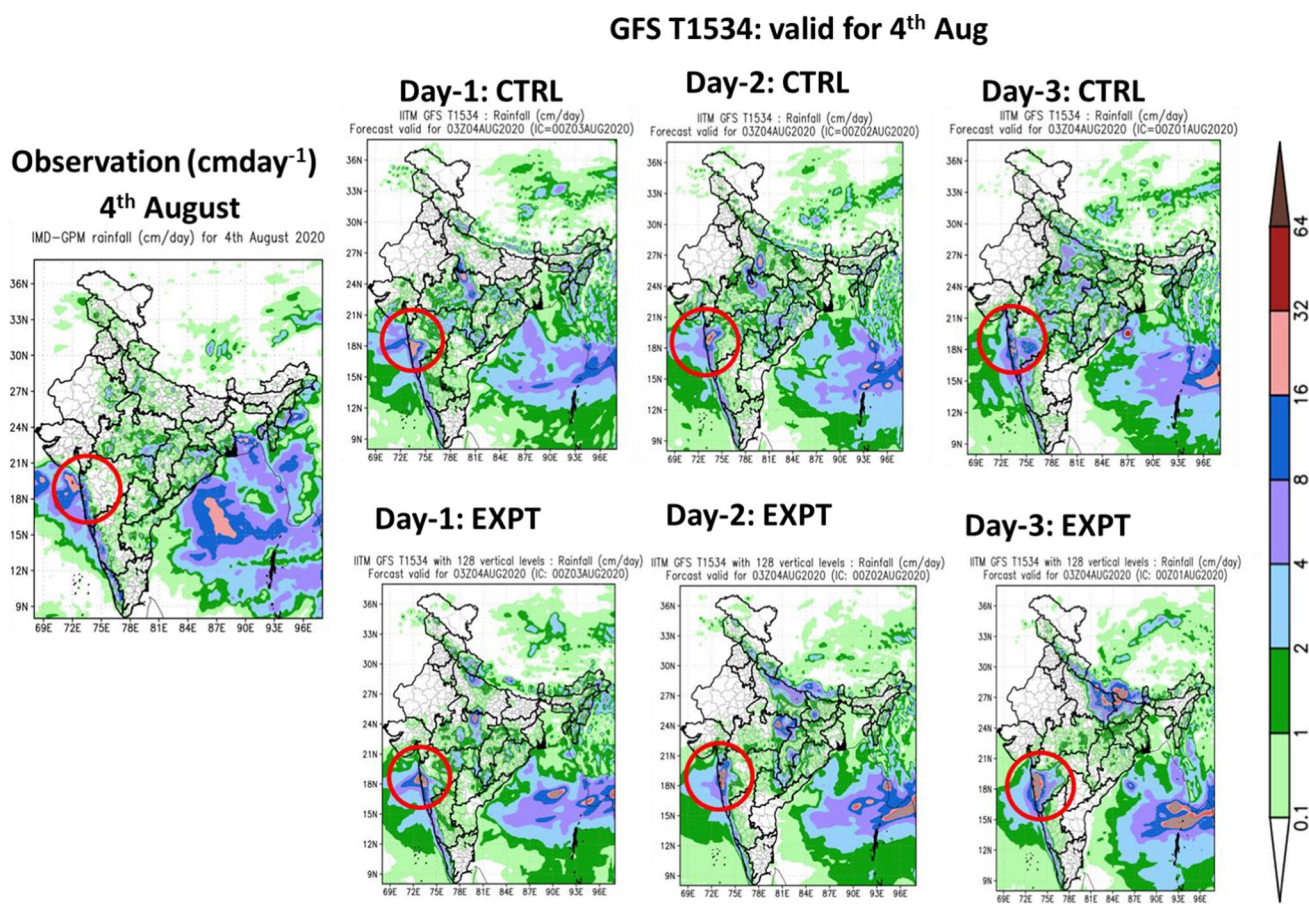

Fig.16 Spatial rainfall (cm day^{-1}) distribution over Mumbai and adjacent region (red circle) reported on 04th August 2020 from IMD-GPM observed merged data. Similar precipitation distribution from CTRL and EXPT valid for 4th August 2020 with day-1, day-2 and day-3 lead time are also shown
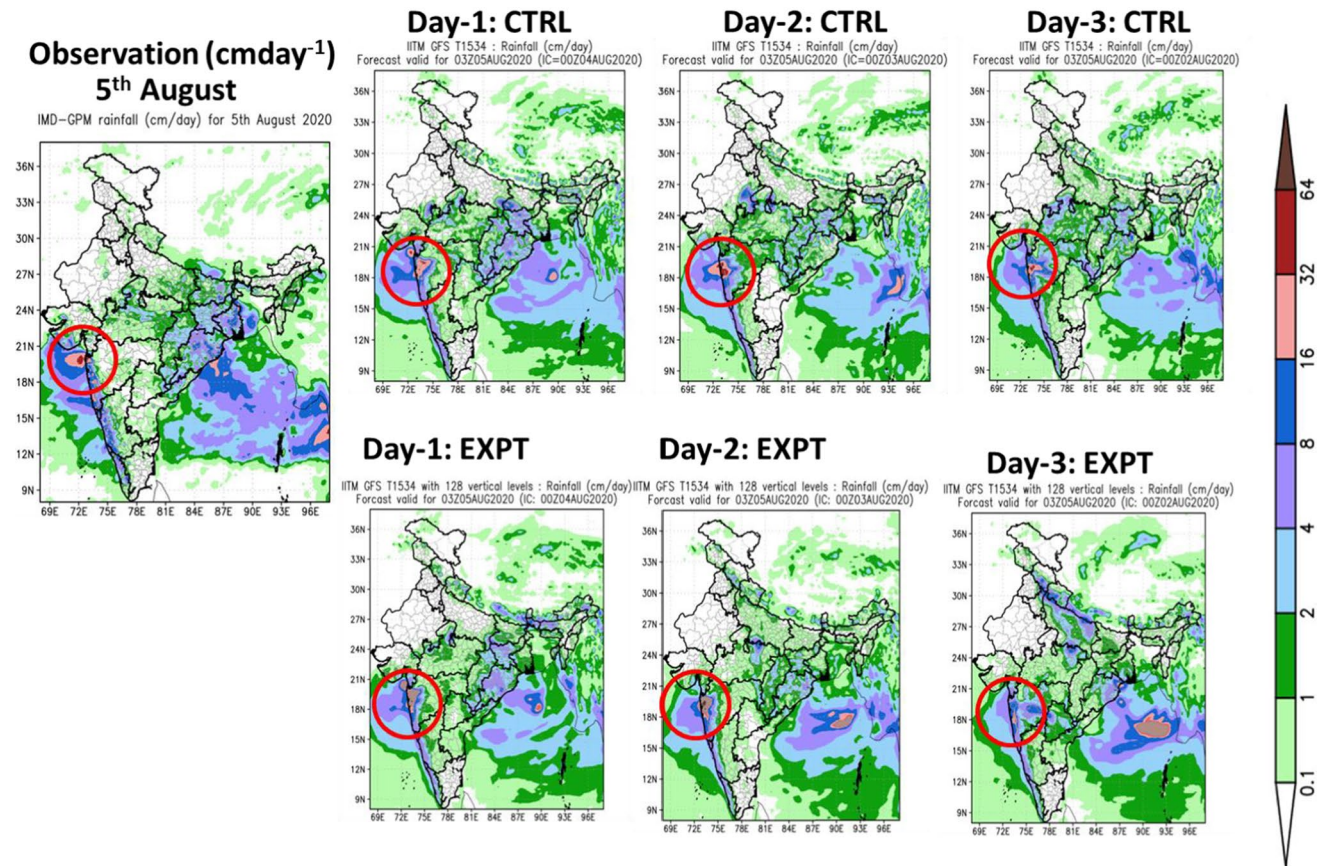
Fig.17 Spatial rainfall (cm day^{-1}) distribution over Mumbai and adjacent region (red circle) reported on 05th August 2020 from IMD-GPM observed merged data. Similar precipitation distribution from CTRL and EXPT valid for 5th August 2020 with day-1, day-2 and day-3 lead time are also shown

with enhanced intensity, further case studies are required to establish its forecast skill over the Indian region.

While the year 2020 monsoon was above normal (109%) according to IMD (https://internal.imd.gov.in/press_release/20201220_pr_963.pdf), the skill of the below normal monsoon year (2018; https://mausam.imd.gov.in/jaipur/mcdata/monsoon2018.pdf) and associated extreme rainfall are also assessed (Figure not shown). It is found that there is a slight different precipitation distribution with slightly degraded skills score over central India region in EXPT than CTRL as compared to the year of 2020. However, EXPT shows the potential in predicting better intensity of the heavy rainfall event as compared to CTRL forecast for below normal monsoon year (2018). Although to reach a statistically significant skill score, more number of years of forecast run with enhanced vertical resolution model are required. However, due to the present limitation of our computational facility, it is difficult to carry out forecast run with large number of years with contrasting monsoonal rainfall. It

will be carried out in future study based on the availability of computational resources.

The present manuscript brings out the sensitivity of enhanced vertical resolution in the current operational weather forecast model GFS T1534 on the forecast of the Indian summer monsoon for 2020. It is noted that EXPT performed reasonably well in forecasting precipitation over most of the Indian subcontinent except the northeast India, Himalayan foothills, WGs, and BOB region. As CI is considered the core monsoon zone (Rajeevan et al. 2010), the enhanced forecast skill over the region is likely to be beneficial for the agricultural and associated socio-economic activity. However, further efforts are required to improve the model forecast over the other region, which is kept for future study. Additionally, it would be worth investigating the impact of the enhanced vertical resolution model in predicting the intensity and track of tropical cyclones during pre-monsoon and post-monsoon seasons.
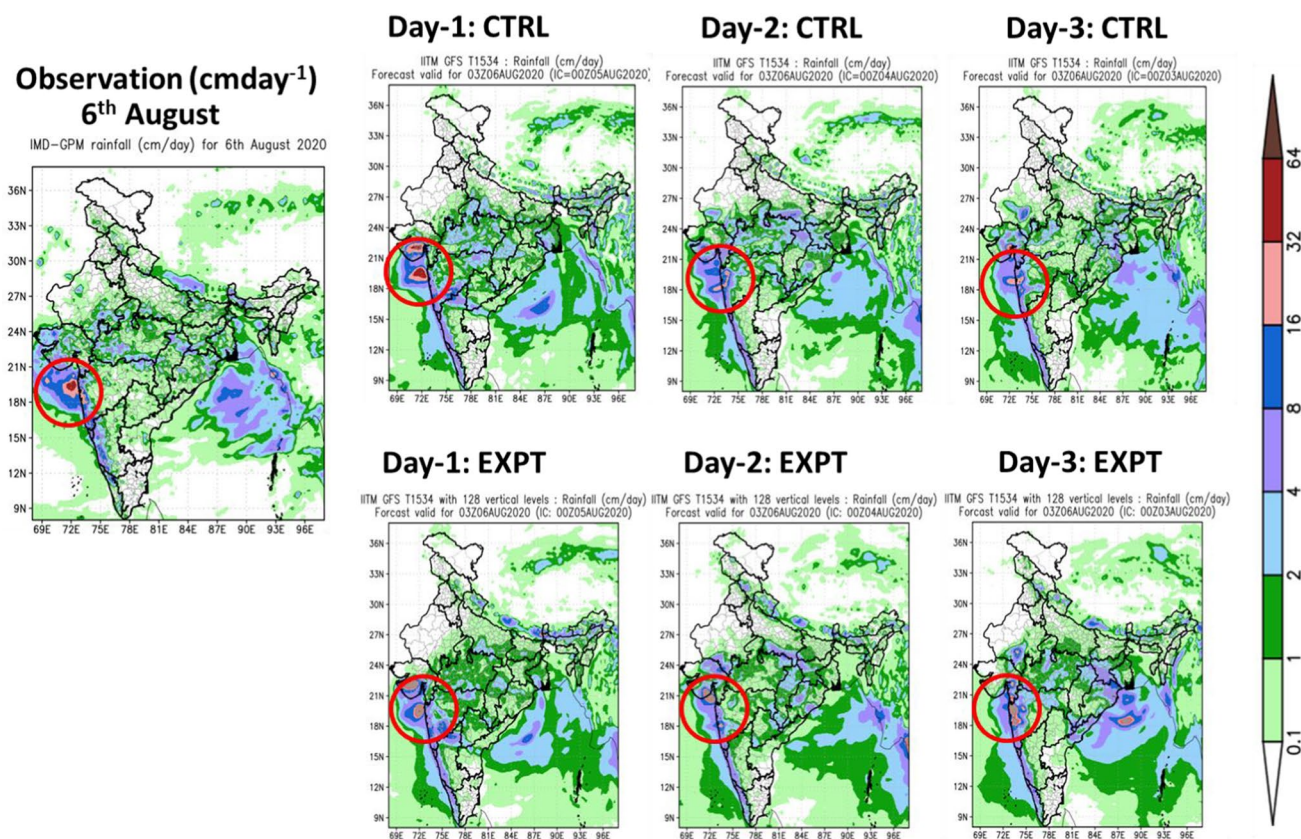
Fig.18 Spatial rainfall (cm day^{-1}) distribution over Mumbai and adjacent region (red circle) reported on 06th August 2020 from IMD-GPM observed merged data. Similar precipitation distribution from CTRL and EXPT valid for 6th August 2020 with day-1, day-2 and day-3 lead time are also shown
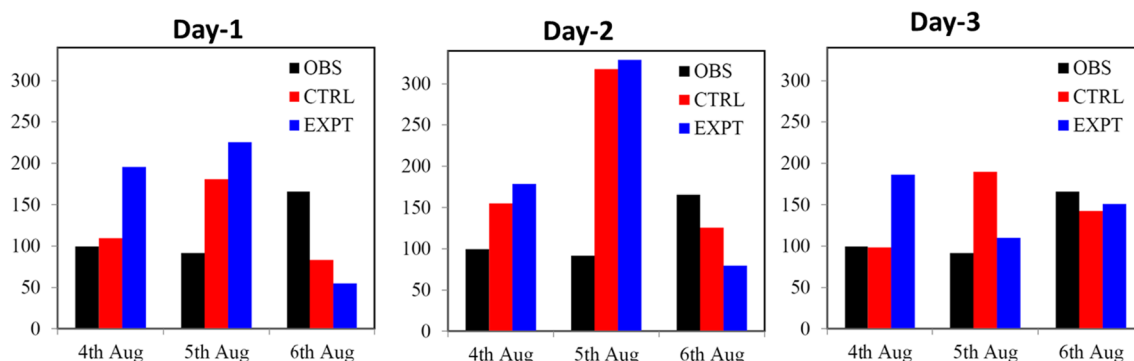

Fig.19 The amount of precipitation (mm day^{-1}) over Mumbai and surrounding regions (72.5°E-73.5°E, 18.5°N-19.5°N) during 4th to 6th August 2020 from observation (black bar), CTRL (red bar) and EXPT (blue bar) for day-1, day-2 and day-3 lead time

4 Conclusions

The present manuscript investigates the sensitivity of enhanced vertical resolution in the operational short to medium-range weather forecast model (GFS T1534) over the Indian summer monsoon region during JJAS of the year 2020. The vertical resolution of the present GFS is increased from L64 to L128 hybrid vertical layers with model top level of 0.27 hPa (~ 54 km) and 0.01 hPa (80 km), respectively. The horizontal resolution of both the models is 12.5 km. To find out the influence of enhanced vertical resolution, two separate forecast runs are carried

out with GFS T1534 with L64 (CTRL) and L128 (EXPT) during JJAS of the year 2020. Except for the difference in the vertical resolution, all the other model components are the same in both models. The model forecast evaluation indicates that EXPT shows improved precipitation distribution over the CI, Indo-Gangetic plains, and southern peninsula regions over the CTRL forecast. However, EXPT shows a considerable overestimation of rainfall over the northeast India, Himalayan foothills, WGs, and BOB region compared to both observation and CTRL. This is one of the major issues with the EXPT forecast, which needs detailed investigation. Preliminary analyses show that enhanced vertical resolution over the above mountainous region leads to enhanced vertical velocity and associated moisture convergence, which helps get excess rainfall over those areas. Apart from the above regions, the precipitation distribution over the central Indian landmass region shows improvement in rainfall PDF and CDF distribution. The heavy to very heavy and extreme rainfall distribution has improved in EXPT compared to the CTRL forecast for all the lead time during JJAS of 2020. However, the lighter category rainfall is overestimated in EXPT forecast. The realistic distribution of convective and large-scale rainfall in the EXPT forecast supports the improved rainfall distribution over the CI region.

The large-scale local Hadley circulation is predicted by both CTRL and EXPT forecasts with slightly stronger mid-level upward motion over the Indian landmass region. Consequently, both models show marginal overestimation of mid-level relative humidity in the atmospheric column with slightly better distribution in EXPT compared to the CTRL. Further, EXPT indicates relatively improved lower-level moisture distribution over the Indian landmass region compared to the CTRL forecast. Additionally, the model skill score based on precipitation suggests that EXPT shows better Bias and ETS skill scores over the CI region than the CTRL forecast. Particularly, the improved ETS for heavier category rainfall is noteworthy in the EXPT forecast. However, the precipitation forecast skill degrades over Indian subcontinent region in EXPT forecast compared to CTRL. The above results possibly suggest that increasing vertical resolution alone may not be sufficient in improving the overall model performance. The model's physical schemes should be tuned for the higher vertical resolution model as the closure assumption of a physical scheme has been tested in relatively low-vertical resolution model. Additionally, as the model top is upraised, new physics (such as gravity wave drag and radiation effect of ozone) may be necessary for the model.

The impact of enhanced vertical resolution in forecasting the diurnal cycle of precipitation is also investigated in the present study based on 3-hourly observation and model data. The spatial distribution of rainfall at 3-hourly intervals starting from 0230 to 2330 IST indicates improved distribution in EXPT over that of CTRL forecast. However, gross overestimation of precipitation is noted over the northeast India, Himalayan foothills and WGs region in EXPT, which is eventually added up in daily scale. The diurnal precipitation cycle over CI shows that the EXPT forecast can predict the phase and magnitude of rainfall realistically compared to observation. On the other hand, CTRL shows precipitation peaks 3-h earlier than observation with an enhanced magnitude over CI. Additionally, it is found that both models fail to capture the diurnal cycle over the northeast and northwest India region due to its inability to capture the local dynamics and thermodynamical properties.

The case study based on extreme rainfall over Mumbai and the surrounding region suggests that EXPT shows potential in predicting extreme rainfall with enhanced intensity and longer lead times compared to the CTRL forecast. It is able to retain the intensity of heavy rainfall for longer lead times. Based on all the above results, it is found that the GFS T1534 L128 (EXPT) model forecast demonstrated better fidelity in forecasting precipitation over the CI region than the CTRL forecast. However, further improvement is required to address the excess precipitation issue over the northeast India, Himalayan foothills, WGs, and BoB region. In addition, it would be interesting to investigate in a future study the impact of enhanced vertical resolution in GFS on the prediction of tropical cyclone track and intensity over the ISM domain.

Author contributions P. Mukhopadhyay, R. Phani Murali Krishna and Malay Ganai conceptualized the work. Material preparation, data collection and analysis were performed by Malay Ganai and Snehlata Tirkey. The first draft of the manuscript was written by Malay Ganai, Snehlata Tirkey, and R. Phani Murali Krishna. Review and editing done by P. Mukhopadhyay. All authors read and approved the final manuscript.

Data availability The datasets generated during and/or analysed during the current study are available in the "Pratyush" high performance computing system at IITM, Pune, India and can be made available by request to the corresponding author.

Declarations

Competing interests The authors have no relevant financial or non-financial interests to disclose. However, due to conflict of interest, the paper may not be sent to scientists of IITM, Pune for peer review process.

References

Abhik S, Mukhopadhyay P, Goswami BN (2014) Evaluation of mean and intraseasonal variability of Indian summer monsoon simulation in ECHAM5: identification of possible source of bias. Clim Dyn 43:389–406. https://doi.org/10.1007/s00382-013-1824-7

Alpert JC, Kanamitsu M, Caplan PM, Sela JG, White GH, Kalnay E (1988) Mountain induced gravity wave drag parameterization in the NMC MRF model. Proceedings of the Eighth Conference on Numerical Weather Prediction, Baltimore, MD. Am Meteorol Soc 8:726–733

Barde V, Nageswararao MM, Mohanty UC, Panda RK, Ramadas M (2020) Characteristics of southwest summer monsoon rainfall events over East India. Theor Appl Climatol 141:1511–1528. https://doi.org/10.1007/s00704-020-03251-y

Bauer et al (2013) Model cycle 38r2: Components and performance. ECMWF Tech. Memo. 704 ECMWF Reading United Kingdom 58 pp. https://www.ecmwf.int/sites/default/files/elibrary/2013/7986-model-cycle-38r2-components-andperformance.pdf

Bhaskar Rao DV, Hari Prasad D, Srinivas D, Anjaneyulu Y (2010) Role of vertical resolution in numerical models towards the intensification, structure and track of tropical cyclones. Mar Geod 33:338–355. https://doi.org/10.1080/01490419.2010.518066

Charron M et al (2012) The stratospheric extension of the Canadian global deterministic medium-range weather forecasting system and its impact on tropospheric forecasts. Mon Wea Rev 140:1924–1944. https://doi.org/10.1175/MWRD-11-00097.1

Chen SS, Houze RA (1997) Diurnal variation and life-cycle of deep convective systems over the tropical Pacific warm pool. Q J R Meteorol Soc 123:357–388

Chun H-Y, Baik J-J (1998) Momentum flux by thermally induced internal gravity waves and its approximation for largescale models. J Atmos Sci 55:3299–3310

Dai AF, Trenberth KE (2004) The diurnal cycle and its depiction in the Community Climate System Model. J Clim 17:930–995

Gadgil S, Gadgil S (2006) The Indian monsoon, GDP and agriculture. Econ Polit Week 41:4887–4895

Ganai M, Krishna RPM, Mukhopadhyay P, Mahakur M (2016) The impact of revised simplified Arakawa-Schubert scheme on the simulation of mean and diurnal variability associated with active and break phases of Indian Summer Monsoon using CFSv2. J Geophys Res Atmos 121:9301–9323. https://doi.org/10.1002/2016JD025393

Ganai M, Tirkey S, Krishna RPM, Mukhopadhyay P (2021) The impact of modified rate of precipitation conversion parameter in the convective parameterization scheme of operational weather forecast model (GFS T1534) over Indian summer monsoon region. Atmos Res 248:105185. https://doi.org/10.1016/j.atmosres.2020.105185

Goswami BN, Venugopal V, Sengupta D, Madhusoodanan MS, Xavier PK (2006) Increasing trend of extreme rain events over India in a warming environment. Science 314(5804):1442–1445. https://doi.org/10.1126/science.1132027

Hack JJ, Caron JM, Danabasoglu G, Oleson KW, Bitz C, Truesdale J (2006) CCSM–CAM3 climate simulation sensitivity to changes in horizontal resolution. J Clim 19:2267–2289

Han J, Pan H-L (2011) Revision of convection and vertical diffusion schemes in the NCEP global forecast system. Weather Forecast 26(4):520–533. https://doi.org/10.1175/WAF-D-10-05038.1

Han J, Witek ML, Teixeira J, Sun R, Pan H, Fletcher JK, Bretherton CS (2016) Implementation in the NCEP GFS of a Hybrid Eddy-Diffusivity Mass-Flux (EDMF) Boundary Layer Parameterization with Dissipative Heating and Modified Stable Boundary Layer Mixing. Wea Forecasting 31:341–352. https://doi.org/10.1175/WAF-D-15-0053.1

Han J, Wang W, Kwon YC, Hong S-Y, Tallapragada V, Yang F (2017) Updates in the NCEP GFS cumulus convection schemes with scale and aerosol awareness. Weather Forecast 32(5):2005–2017. https://doi.org/10.1175/WAF-D-17-0046.1

Hersbach H, Dee D (2016) ERA5 reanalysis is in production. In: ECMWF Newsletter No. 147 p 7. https://www.ecmwf.int/en/newsletter/147/news/era5-reanalysis-production

Huffman GJ, Stocker EF, Bolvin DT, Nelkin EJ, Jackson Tan (2019) GPM IMERG Final Precipitation L3 Half Hourly 0.1 degree x 0.1 degree V06, Greenbelt, MD, Goddard Earth Sciences Data and Information Services Center (GES DISC). https://doi.org/10.5067/GPM/IMERG/3B-HH/06, https://disc.gsfc.nasa.gov/datasets/GPM_3IMERGHH_06/summary?keywords%20=%20IMERG. Accessed 20 Dec 2021

Kiehl JT, Williamson DL (1991) Dependence of cloud amount on horizontal resolution in the National Center for Atmospheric Research Community Climate Model. J Geophys Res 96(10 955–):10 980

Kim Y-J, Arakawa A (1995) Improvement of orographic gravity wave parameterization using a mesoscale gravity wave model. J Atmos Sci 52:1875–1902

Lee E, Lee E, Choi I (2019) Impact of increased vertical resolution on medium-range forecasts in a global atmospheric model. Mon Weather Rev 147:4091–4106

Lindzen RS, Fox-Rabinovitz M (1989) Consistent vertical and horizontal resolution. Mon Wea Rev 117:2575–2583

Lott F, Miller MJ (1997) A new subgrid scale orographic drag parameterization: Its formulation and testing. QJRMS 123:101–127

Mahlman JD, Umscheid LJ (1987) Comprehensive modeling of the middle atmosphere: the influence of resolution. In: Visconti G, Garcia R (eds) Transport Process in the Middle Atmosphere. D. Reidel, Hingham, MA, pp 251–266

Manganello JV, Hodge KI, Kinter JL et al (2012) Tropical cyclone climatology in a 10-km global atmospheric GCM: toward weather-resolving climate modeling. J Clim 25:3867–3893

Mass CF, Ovens D, Westrick K, Colle BA (2002) Does increasing horizontal resolution produce more skillful forecasts? Bull Amer Meteor Soc 83:407–430. https://doi.org/10.1175/1520-0477(2002)083%3c0407:DIHRPM%3e2.3.CO;2

Mitra AK, Prakash S, Imranali MM, Pai DS, Srivastava AK (2014) Daily merged satellite gauge real-time rainfall dataset for Indian Region. Vayumandal 40(1–4):33–43

Mukhopadhyay P et al (2019) Performance of a very high-resolution global forecast system model (GFS T1534) at 12.5 km over the Indian region during the 2016–2017 monsoon seasons. J Earth Syst Sci 128:1–18. https://doi.org/10.1007/s12040-019-1186-6

Nageswararao MM, Mohanty UC, Ramakrishna SSVS, Nair A, Prasada SK (2016) Characteristics of winter precipitation over Northwest India using high-resolution gridded dataset (1901–2013). Global Planet Change 147:67–85. https://doi.org/10.1016/j.gloplacha.2016.10.017

Pokhrel S, Sikka DR (2012) Variability of the TRMM-PR total and convective and stratiform rain fractions over the Indian region during the summer monsoon. Clim Dyn 41:21–44. https://doi.org/10.1007/s00382-012-1502-1

Prasad VS, Johny CJ, Sodhi JS (2016) Impact of 3D Var GSI-ENKF hybrid data assimilation system. J Earth Syst Sci 125(8):1509–1521

Rajeevan M, Bhate J, Jaswal AK (2008) Analysis of variability and trends of extreme rainfall events over India using 104 years of gridded daily rainfall data. Geophys Res Lett 35:L18707. https://doi.org/10.1029/2008GL035143

Rajeevan M, Gadgil S, Bhate J (2010) Active and break spells of the Indian summer monsoon. J Earth Syst Sci 119:229–247

Roxy MK, Ghosh S, Pathak A, Athulya R, Mujumdar M, Murtugudde R et al (2017) A threefold rise in widespread extreme rain events over Central India. Nat Commun 8(1):708. https://doi.org/10.1038/s41467-017-00744-9

Ruti PM, Rocco DD, Gualdi S (2006) Impact of increased vertical resolution on simulation of tropical climate. Theor Appl Climatol 85:61–80. https://doi.org/10.1007/s00704-005-0174-8

Sabeerali CT, Rao SA, Dhakate AR et al (2015) Why ensemble mean projection of south Asian monsoon rainfall by CMIP5 models is not reliable? Clim Dyn 45:161–174. https://doi.org/10.1007/s00382-014-2269-3

Sahany S, Venugopal V, Nanjundiah RS (2010) Diurnal-scale signatures of monsoon rainfall over the Indian region from TRMM satellite observations. J Geophys Res 115:D2. https://doi.org/10.1029/2009JD012644

Sela J (2010) The derivation of sigma pressure hybrid coordinate semi-Lagrangian model equations for the GFS. In: NCEP Office Note 462:1–31. https://repository.library.noaa.gov/view/noaa/6971

Sen Roy S, Balling RC Jr (2004) Trends in extreme daily precipitation indices in India. Int J Climatol 24:457–466. https://doi.org/10.1002/joc.995

Sui C-H, Lau K-M, Takayabu YN, Short DA (1997) Diurnal variations in tropical oceanic cumulus convection during TOGA COARE. J Atmos Sci 54:639–655

Sundqvist H, Berge E, Kristjansson JE (1989) Condensation and cloud parameterization studies with a mesoscale numerical weather prediction model. Mon Weather Rev 117:1641–1657. https://doi.org/10.1175/1520-0493(1989)117%3c1641:CACPSW%3e2.0.CO;2

Wilks DS (2011) Statistical methods in atmospheric sciences, 3rd edn. International Geophysics Series, No. 100, Academic Press, USA, 669 pp

Yanai M, Esbensen S, Chu J-H (1973) Determination of bulk properties of tropical cloud clusters from large-scale heat and moisture budgets. J Atmos Sci 30:611–627. https://doi.org/10.1175/1520-0469(1973)030%3c0611:DOBPOT%3e2.0.CO;2

Yang GY, Slingo J (2001) The diurnal cycle in the tropics. Mon Weather Rev 129:784–801

Zhang D-L, Wang X (2003) Dependence of hurricane intensity and structures on vertical resolution and time-step size. Adv Atmos Sci 20:711–725. https://doi.org/10.1007/BF02915397

Zhao Q, Carr FH (1997) A prognostic cloud scheme for operational NWP models. Mon Weather Rev 125(8):1931–1953. https://doi.org/10.1175/1520-0493(1997)125%3c1931:APCSFO%3e2.0.CO;2